Summer 2019

Under what conditions could eelgrass measurably drawdown carbon? Relating carbon drawdown to pCO2, irradiance, and leaf area index of Zostera marina

Tyler Tran
Western Washington University, tyler.tran@wwu.edu

Under what conditions could eelgrass measurably drawdown carbon? Relating carbon drawdown to pCO_2, irradiance, and leaf area index of *Zostera marina*

By

Tyler Tran

In Partial Completion of

the Requirements for the Degree

Master of Science

ADVISORY COMMITTEE

Dr. Brooke Love, Chair

Dr. Sylvia Yang

Dr. Brian Bingham

GRADUATE SCHOOL

David L. Patrick, Interim Dean

Master's Thesis

In presenting this thesis in partial fulfillment of the requirements for a master's degree at Western Washington University, I grant to Western Washington University the non-exclusive royalty-free right to archive, reproduce, distribute, and display the thesis in any and all forms, including electronic format, via any digital library mechanisms maintained by WWU.

I represent and warrant this is my original work, and does not infringe or violate any rights of others. I warrant that I have obtained written permissions from the owner of any third party copyrighted material included in these files.

I acknowledge that I retain ownership rights to the copyright of this work, including but not limited to the right to use all or part of this work in future works, such as articles or books.

Library users are granted permission for individual, research and non-commercial reproduction of this work for educational purposes only. Any further digital posting of this document requires specific permission from the author.

Any copying or publication of this thesis for commercial purposes, or for financial gain, is not allowed without my written permission.

Tyler Tran

August 15th, 2019

Under what conditions could eelgrass measurably drawdown carbon?
Relating carbon drawdown to pCO_2, irradiance, and leaf area index of *Zostera marina*

A Thesis
Presented to
The Faculty of
Western Washington University

In Partial Fulfillment
Of the Requirements for the Degree
Master of Science

By
Tyler Tran
August - 2019

Abstract

Seagrass meadows, common to coastal habitats, have been identified as potential short-term refugia for calcifying organisms from ocean acidification (OA). In nearshore, soft-sediment habitats of the Salish Sea, eelgrass (*Zostera marina* L.) is the dominant seagrass species, and several studies have found that eelgrass is effective at taking up inorganic carbon and may be carbon-limited, potentially increasing uptake potential in the future. However, irradiance levels vary throughout a day and can therefore influence rates of carbon uptake and release through the relative rates of photosynthesis and respiration. Eelgrass meadows vary in terms of meadow size, shoot density and morphology, and water residence time which could affect rates of carbon uptake of eelgrass meadows and their influence on localized water chemistry. We conducted a series of mesocosm experiments manipulating pCO_2, irradiance, and leaf area index (LAI) to assess how these factors interact and contribute to OA variability in the nearshore environment. Our findings demonstrate that increased pCO_2 may release the eelgrass from carbon limitation and increase carbon uptake rates. The effect of increased pCO_2 on eelgrass carbon uptake was only evident at high irradiance, and high LAI. While greater shoot density increased overall carbon uptake, this effect may diminish as self-shading and/or carbon limitation brought on by photosynthetic carbon uptake emerge at high density. Therefore, eelgrass meadows could potentially measurably drawdown carbon but only when eelgrass with sufficiently high LAI is exposed to saturating irradiance conditions with relatively long water residence times and/or with shallow water depth. We identified rates of carbon uptake and rates of pH increase as a function of LAI. This information will help natural resource managers understand variability of OA due to the photosynthetic activity of eelgrass in meadows throughout the Salish Sea.

Acknowledgements

First and foremost, I thank my advisor, Dr. Brooke Love, for her endless advising, support and expertise in marine chemistry. She has provided me with a learning opportunity to work independently and has also been there to collaborate when needed. I also thank my committee members, Dr. Sylvia Yang and Dr. Brian Bingham, who have provided their expertise in seagrass biology and statistical analysis. I would not be where I am today without the support of my committee and all of those who have helped me along the way. I thank Brooke McIntyre, Mike Adamczyck, Cristina Villalobos, Lynne Nowak, Hillary Thalmann, Katey Williams, Jayshen Blows, Eric Wilson, Abby Ernest-Beck, Darby Finnegan, Michelle Tanz, and Faythe Duran, for help with many different parts of the research process. Morgan Eisenlord also helped me conduct the leaf area index surveys. I would also like to thank the facilities management at Shannon Point Marine Center for technical and materials support. Capt. Nate Schwark, Andy Wilken, Joyce Foster, Horng-Yuh Lee, and Gene McKeen, you all make SPMC a dream place to work.

I also couldn't have dedicated the necessary time towards research if it wasn't for funding sources including the WA Dept. of Natural Resources, Huxley College, Padilla Bay Foundation, and the Northwest Climate Adaptation Science Center. I sincerely thank anyone who has supported me through this accomplishment.

Table of Contents

List of Figures

List of Tables

Introduction

Anthropogenic carbon dioxide (CO_2) emissions have increased the concentration of atmospheric CO_2 and are projected to continue rising (IPCC 2014). Pre-industrial concentrations of atmospheric CO_2 (1750-1850) were approximately 280 ppm (Caldeira and Wickett 2005); however, present atmospheric CO_2 concentrations have reached more than 400 ppm (NOAA 2016) and are expected to continue increasing to 1000 ppm by 2100 (Meehl et al. 2007, Fabry et al. 2008, IPCC 2014). As atmospheric CO_2 increases, so does the partial pressure of CO_2 (pCO_2) which drives the diffusion of atmospheric CO_2 into the ocean. Increasing pCO_2 has led to approximately 30% of the anthropogenic CO_2 to be absorbed in the ocean since the pre-industrial era (Caldeira and Wickett 2003, Orr et al. 2005, Feely et al. 2009, IPCC 2014).

As atmospheric CO_2 is absorbed in the ocean, a series of chemical reactions occurs that result in ocean acidification (OA) which can have negatively impact calcifying organisms (Royal Society 2005). Absorption of atmospheric CO_2 in the ocean shifts the chemical equilibria of the marine carbonate system (pCO_2, pH, dissolved inorganic carbon, and aragonite saturation state) toward increased pCO_2, decreased pH, increased dissolved inorganic carbon concentrations, and decreased aragonite saturation state (Ω_{Ar}) (Orr et al. 2005). In the open ocean, surface seawater pH has decreased by 0.11 pH units (compared to pre-industrial levels of approximately 8.21 to 8.1 pH units) and is expected to continue to decrease by 0.3-0.4 additional pH units by 2100 (Caldeira & Wickett 2005, Orr et al. 2005, Solomon et al. 2007). The carbonate chemistry equilibrium shift also favors decreased carbonate ion (CO_3^{2-}) making it more difficult for organisms to calcify since calcium carbonate ($CaCO_3$) is more soluble under these conditions (Iglesias-Rodriguez et al. 2008, Ries et al. 2008, Kroeker et al. 2010). The $CaCO_3$ saturation state (Ω) is a measure of CO_3^{2-} concentration relative to water in equilibrium with the two forms of solid calcium carbonate minerals, calcite and

aragonite, and the dissolution of calcium carbonate minerals is physically favored when its value is less than one. Ocean acidification has a greater effect on the aragonite saturation state (Ω_{Ar}) because aragonite is more soluble than calcite under similar conditions (Mucci, 1983). Furthermore, since many shellfish larvae use primarily aragonite to build their shells (Palmer 1992, Iglesias-Rodrıguez et al. 2008, Ries et al. 2008, Kroeker et al. 2010), OA is especially detrimental to early life stages of shellfish. An aragonite saturation state (Ω_{Ar}) of 1.2 to 1.5 can compromise biogenic calcification of larval Pacific oysters, leading to increased mortality (Waldbusser et al. 2015, Guinotte and Fabry 2008). Some of the most pronounced effects of OA are on calcifying organisms, but it also has influences other organisms and biological and physiological processes in widely varying taxa (Hinga 2002, Wootton et al. 2008, Hale et al 2011, Kroeker et al. 2013, Busch and McElhany 2016). Studies specific to the Salish Sea region predict a general decrease in crustacean and mollusks productivity (especially copepods, small crustaceans, and benthic grazers) and increase in soft infauna, suspension feeders, and small gelatinous plankton (Busch, Harvey, and McElhany 2013).

In addition to predicted decreases in pH due to anthropogenic CO_2, the Salish Sea experiences periodic wide swings in pH due to coastal and estuarine processes. Along the West Coast of the United States, seasonal upwelling can deliver pCO_2 enriched water from the deep ocean into shallow coastal habitats from April to November, producing pH swings of approximately -0.4 pH units compared to ambient surface waters (Feely et al. 2008). This level of pH variation is of a scale larger than changes predicted to occur by 2100 in the open ocean due to anthropogenic CO_2 alone (Feely et al. 2008). Parts of the Salish Sea can experience acidification from coastal upwelling because tidal and estuarine circulation processes transport acidified seawater from the coast to the estuary (Feely et al. 2010). In addition to anthropogenic CO_2 and coastal upwelling, heterotrophic respiration of organic matter is a dominant estuarine process that increases pCO_2 values in the ocean (Hedges et al.

1997, Frankignoulle et al. 1998, Borges and Frankignoulle 1999, Cai et al. 1999). Observations of heterotrophic respiration has led to a pH decrease by 0.24 units in Hood Canal (Feely et al. 2010). Therefore, the decrease pH driven by anthropogenic CO_2 is in addition to present coastal and estuarine processes that control pH conditions in the Salish Sea.

Upwelling events have led to decreased recruitment of oyster larvae along the west coast, and several shellfish hatcheries have adapted their strategies to manage episodic low pH and low Ω_{Ar} events (Barton et al. 2012). These hatcheries currently experience seawater conditions that can range from approximately 0.8 to 3.2 Ω_{Ar} and approximately 7.6 to 8.2 pH and they adjust pH levels by adding sodium carbonate to buffer OA when they experience large declines in larval recruitment (Harris et al. 2013, Barton et al. 2015). However, wild stocks of shellfish are subject to natural variation in ocean carbonate chemistry. For example, in Willapa Bay, Washington, pacific oyster larval recruitment has shown long-term declines, potentially due to increasingly acidified seawater brought to the shallows by seasonal upwelling (Dumbauld et al. 2011).

Seagrass meadows may act as potential OA refuges for calcifying organisms. Seagrasses draw down total CO_2 (TCO_2) from the water column during photosynthesis and can therefore reverse OA (Beer and Rehnberg 1997). For example, Unsworth et al. (2012) found that in the field, uptake of inorganic carbon by tropical seagrasses increased seawater pH by 0.38 and increased Ω_{Ar} by 2.9 over a 24-hour residence time and at 1m depth, which are typical conditions of these systems (Black et al. 1990). It was estimated that calcification by scleractinian coral adjacent to seagrass meadows could be enhanced by approximately 18% compared to areas without seagrasses (Manzello et al. 2012, Unsworth et al. 2012). Thus, photosynthetic activity in tropical seagrass meadows could ameliorate OA conditions and increase resilience of calcifying organisms to OA.

In northern temperate estuaries like the Salish Sea, eelgrass (*Zostera marina* L.) is the dominant seagrass species (Christaen et al. 2016), but the ability of eelgrass (*Zostera marina* L.) to modify carbonate chemistry depends on a complex suite of factors including eelgrass abundance, TCO_2 availability, light availability, water depth, and residence time.

The abundance of eelgrass varies throughout the Salish Sea, which could affect rates of carbon uptake at a meadow scale. The ability of eelgrass to take up carbon may vary between eelgrass meadows since they vary in terms of meadow size (0-3000 ha), density (0 to 450 shoots m^{-2}), and morphology (shoot length = 0 to ~200 cm) all of which affect photosynthetic surface area (Phillips et al. 1983, Yang et al. 2013, Christiaen et al. 2016). Meadows with the same biomass per area can be composed of sparsely distributed, large shoots or dense, small shoots (Yang et al. 2013). Furthermore, individual leaves on an eelgrass shoot vary in age and chlorophyll content (Mazzella and Alberte 1986), and presumably photosynthetic capacity. Thus, predicting photosynthetic rates using portions of leaves or individual shoots may not accurately represent the photosynthetic potential of an entire eelgrass meadow. Leaf area index (LAI) functionally summarizes multiple aboveground morphological characteristics into a single abundance metric that represents photosynthetic surface area per area of substrate. Therefore, LAI is appropriate for investigating photosynthetic potential of eelgrass and may provide insight on how photosynthetic rates may translate to eelgrass meadows in the field (Duarte et al. 2010, Echavarria-Heras et al. 2011).

Several studies suggest that eelgrass is carbon-limited and increases its photosynthetic rate under enriched TCO_2 conditions (Zimmerman et al. 1997 Beer and Koch 1996, Thom 1996). An experimental 2-fold increase in pCO_2 (from 280 to 560 μatm) led to increased rates of eelgrass photosynthetic rate by 2.5 times compared to photosynthetic rates of eelgrass at pre-industrial CO_2

conditions under saturating light (Thom 1996). Additionally, greater photosynthetic rates of eelgrass under enriched pCO_2 conditions reduced the daily saturating light requirement (Zimmerman et al. 1997). Another study assessing photosynthetic rates of eelgrass under enriched CO_2 used a six-fold increase in TCO_2 compared to present day and found that photosynthetic rate increased approximately 3-fold (from 2074 to 3673 microequivalents TCO_2 kg^{-1}) (Zimmerman et al. 1997). To put these in context of expected changes, by 2100 in the open ocean, the pCO_2 will be two-fold higher than present day and in upwelling zones near the continental shelf, a pCO_2 increase of approximately 3.5-fold is observed (Feely et al. 2008, IPCC 2014).

Photosynthetic rate of eelgrass varies with light and decreases when light levels are sub-saturating (Olesen and Sand-Jensen 1994, van Lent and Verschuure 1994). Minimum light requirements of eelgrass in the Pacific Northwest, USA is 3 mol quanta m^{-2} day^{-1}, with saturating conditions exceeding 7 mol quanta m^{-2} day^{-1} (Thom et al. 2008). Light limitation determines the maximum depth distribution of eelgrass meadows (Dennison 1987, Duarte 1991, Zimmerman et al. 1991, Zimmerman et al. 1997) and results in seasonal fluctuations in eelgrass growth and abundance (Backman & Barilotti 1976, Barko et al. 1982, Duarte & Kalff 1987, Olesen and Sand-Jensen 1993, Olesen and Sand-Jensen 1994). Maximum shoot density thresholds have been observed in permanent eelgrass meadows due to self-shading of eelgrass leaves (varies seasonally, Olesen and Sand-Jensen 1994). Additionally, light changes drastically over the course of a day and eelgrass meadows can receive about 6 to 8 hours of saturating light (Dennison and Alberte, 1985). Due to minimum requirements for photosynthesis, light that is predominantly sub-saturating has been shown to affect the carbonate chemistry differently than when light is saturating (Zimmerman et al. 1995).

Although several studies have simultaneously investigated photosynthetic rates of eelgrass under different pCO_2 conditions, few studies have investigated how photosynthetic rates could vary amongst eelgrass meadows with different LAIs in a range of light conditions and in a range of pCO_2 conditions that are typical in upwelling and future OA scenarios. In addition to increasing pCO_2 due to burning of fossil fuels, reduced water quality has led to diminished light penetration and has been hypothesized to have caused losses of deep edges of eelgrass meadows (Short and Wyllie-Echeverria 1996). Given concurrent alteration of light availability due to anthropogenic activity in conjunction with anthropogenic CO_2 release, it is necessary to investigate combined drivers to understand the potential of changes in these parameters to influence eelgrass in the Salish Sea and possibly its ability to mitigate ocean acidification.

Because Salish Sea eelgrass meadows can experience ambient variation in pCO_2 and can also self-shade at higher densities, and increase photosynthetic rates at saturating light levels we hypothesize (see Figure 1) that:

> **H_1:** As LAI increases, the overall rate of carbon uptake will remain constant, but will eventually decrease because when there are more leaves present, self-shading will occur.
> **H_{A1}:** The overall rate of carbon uptake will remain constant since self-shading effects will not occur at high LAI
>
> **H_2:** The rate of carbon uptake will increase when initial enrichment of pCO_2 is moderately elevated (under saturating light) since eelgrass have been shown to be carbon limited at ambient pCO_2 conditions (800 μatm).
> **H_{A2}:** Enriched pCO_2 conditions (1800 μatm) will not affect photosynthetic response**.**
>
> **H_3:** Carbon uptake will decrease when light conditions are sub-saturating since there is less light for photosynthesis.
> **H_{A3}:** Sub-saturating light will not affect photosynthetic response.

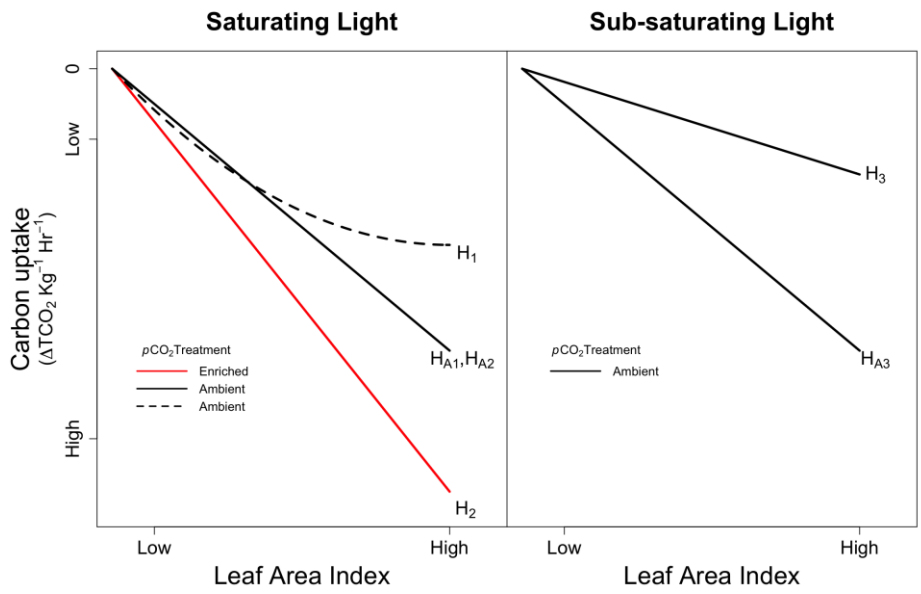

Figure 1. Hypotheses of changes in carbon uptake (ΔTCO_2 per kg^{-1} hr^{-1}) between low and high leaf area index values and between saturating (left panel) and sub-saturating (right panel) light levels. The black dashed line represents self-shading of eelgrass compared to the solid black line (H_1). The black and red lines represent the ambient (800 µatm) and enriched (1800 µatm) pCO_2 treatments respectively (H_2). The red lines in the sub-saturating light treatment represent differences in carbon uptake between light levels (H_3).

In this study, we conducted a series of mesocosm experiments manipulating LAI of whole shoots, pCO_2 levels, and light conditions to assess how these factors interact and contribute to ability of eelgrass to take up carbon and alter pH and the carbonate chemistry system. Mesocosm results can then be extrapolated to make estimates of meadow scale effects. Our study is complementary to other studies that look at the effects of pCO_2 but this study investigates photosynthetic rates of whole shoots and potential self-shading effects at higher densities (also higher LAI). We developed a statistical model from this experiment to quantify rates of carbon uptake of eelgrass under different LAI, pCO_2, and light conditions. The statistical model was used to create a predictive model that also incorporates residence time or water depth. These models may help resource managers identify the drivers of variability in eelgrass meadows throughout the Salish Sea and assess to what extent they could measurably take up carbon.

Methods

Field survey of Leaf Area Index (LAI) and collection of eelgrass

Leaf area index (LAI) is the total leaf area per unit area of substratum (Bulthuis 1990, Solana-Arellano et al. 2003). We conducted a field survey to document the natural variation in LAI of eelgrass meadows in Washington State (Figure 2) by collecting above-ground biomass in quadrats along transects, then measuring leaf area of the biomass sample. We surveyed intertidal eelgrass at seven sites between June and August 2017, using several survey designs, to complement on-going eelgrass monitoring occurring at each site: At Padilla Bay (June, 2017), we collected biomass samples along the Padilla Bay National Estuarine Research Reserve's long term monitoring transects (Stevens et al. 2016). For this monitoring program, 3 permanent transects were oriented perpendicular to shore, each starting at a tidal elevation of +1 m (MLLW) and spanning several kilometers to – 2 m (MLLW). Biomass samples were collected from a 0.0625 m^2 quadrat in each 0.5 m increment of elevation (n=18). At Fidalgo Bay (August, 2017), we collected biomass samples in a 0.25m^2 quadrat (n=12) using the same spacing and layout of the monitoring conducted in Padilla Bay. At Case Inlet, Nisqually Reach, Port Gamble, Skokomish and Willapa Bay (August 2017), eelgrass biomass was collected in 0.0625 m^2 quadrats (n=9) every five meters along transects placed parallel to shore at an elevation of -1m (MLLW).

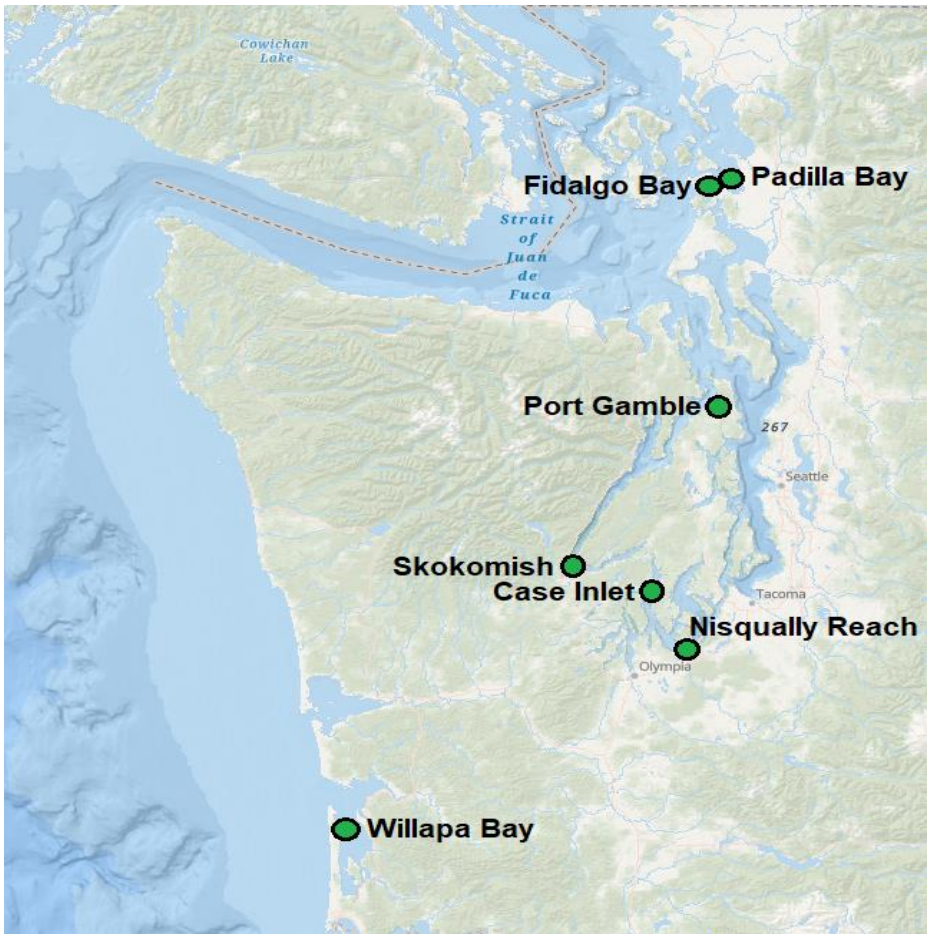

Figure 2. Locations of eelgrass sites for field assessment of leaf area index (LAI) throughout the southern Salish Sea (Washington, USA). Sampling locations are represented by green circles with corresponding site names (Padilla Bay, Fidalgo Bay, Case Inlet, Nisqually Reach, Port Gamble, Willapa Bay, and Skokomish). We sampled 18, 12, 9, 9, 9, 9, and 9 quadrats at the respective sites.

To quantify the total leaf area of each biomass sample, we laid the eelgrass flat, with leaves spread out, on 11"x17" laminate next to a ruler for scale and covered it with transparent acrylic for scanning on a photocopier. Scans were taken in full-color scale, 400 dpi, 11"x17" size, and in JPEG format (Figure 3). The images were converted to black and white so that the pixels of the leaf area was black. Then, the total leaf area was calculated as the total number of black pixels scaled by the number of pixels per centimeter on the ruler, using ImageJ software (Version 1.51t31). The total leaf area from each quadrat was divided by the quadrat area (0.0625 or 0.25 m^2) to calculate leaf area index (LAI) for each sample.

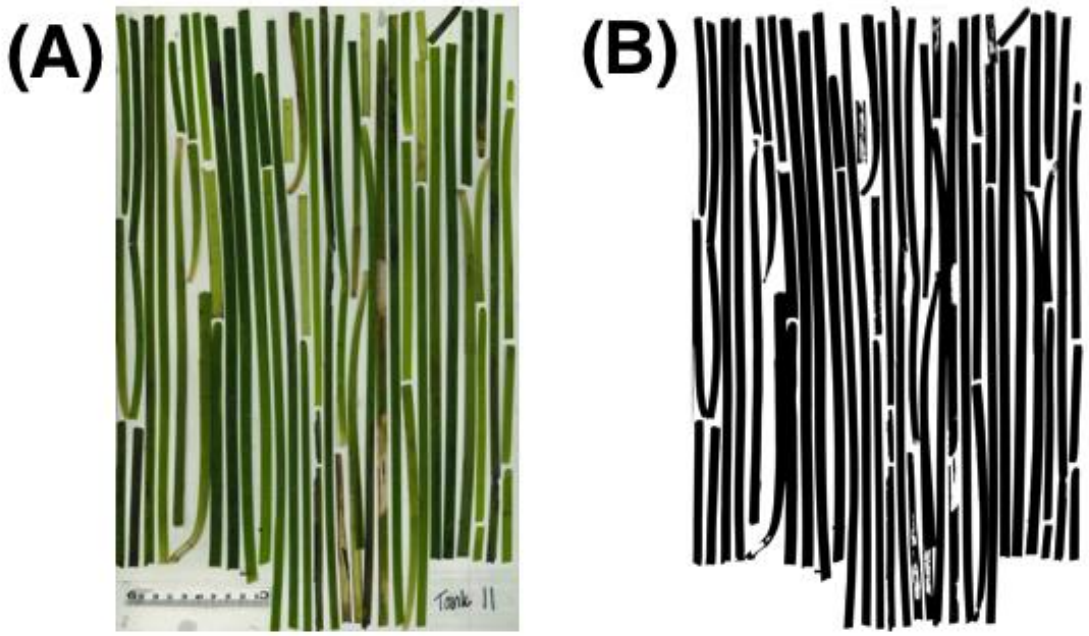

Figure 3. Quantifying the total leaf area of eelgrass to calculate Leaf Area Index (LAI) using (A) a photo copy of eelgrass subsampled from one tank and (B) the same photocopy converted to black and white using ImageJ Software. The software was given the # of pixels per cm using the ruler placed in (A), then the ruler and tank label were removed from the image, and the eelgrass was converted to black pixels to calculate the total area using the total number of pixels.

Mesocosm System and Experimental Design

The mesocosm system consisted of 18 gravity-fed acrylic tanks (44 cm x 21 cm x 39 cm) containing 40 L of seawater (Figure 4). Ambient seawater (800 μatm) was pumped from Guemes Channel (approximately 7 m below mean low water) into a header pipe overflowing at a fixed height for constant head pressure. The header pipe distributed the flow of seawater equally into the tanks. Water overflowed into an outer water jacket around each tank, then to waste. A range of leaf area index (LAI) treatments, two pCO_2 treatments, and three irradiance treatments were randomly assigned to the mesocosm system over three daytime experimental trials and one nighttime trial:

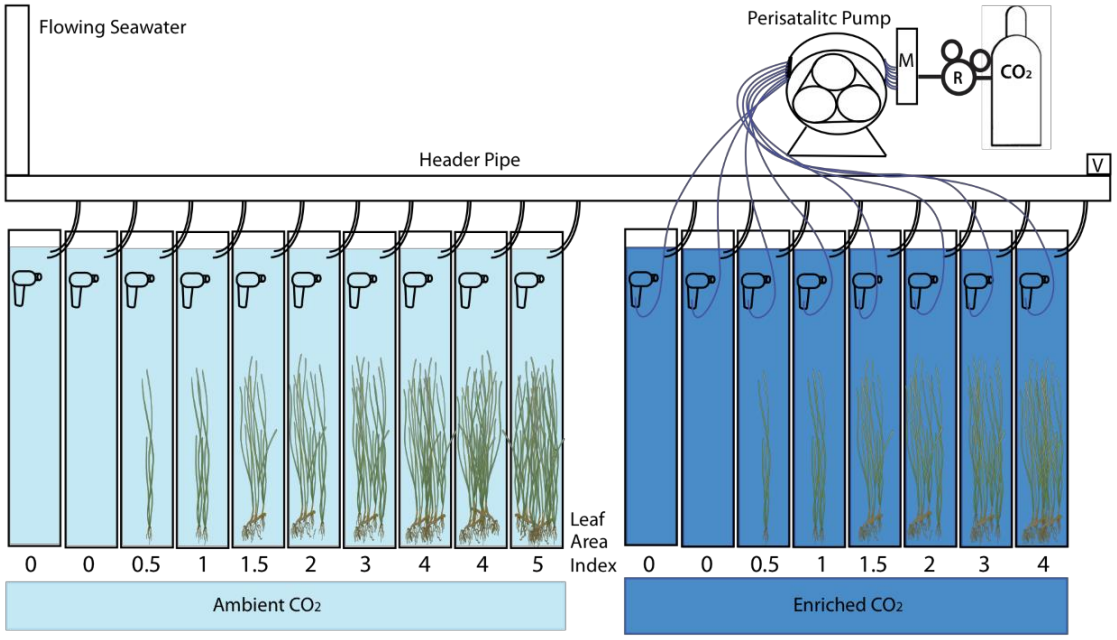

Figure 4. Schematic of mesocosm system for pCO_2 and leaf area index manipulations. Eighteen 40 L experimental tanks, eight tanks were enriched pCO_2 and 10 tanks received ambient pCO_2 water (approximately 2000 and 800 µatm respectively). Target values of LAI ranged from 0-5 for each pCO_2 condition. LAI and pCO_2 treatments were randomized by tank in the actual experiment.

Eelgrass LAI Treatments: Target LAI values ranged from 0 to 5 to mimic the range of LAI values observed in the field. We collected eelgrass for the mesocosm experiment from Padilla Bay, WA: Adult eelgrass (whole shoots) were excavated by hand from Padilla Bay on Nov. 4th, 2017 and immediately transported to Shannon Point Marine Center in Anacortes, WA. The eelgrass was soaked in 15 ppt seawater for one hour to eliminate clinging epifauna and reduce the presence of wasting disease (Carr et al. 2011). The experimental shoots' rhizomes were cut to 6 cm in length, and shoots were acclimated in two indoor holding tanks (72 L) with flowing ambient seawater for two weeks (PAR = 0.55 ± 0.04 mol m^{-2} d^{-1}). Prior to the start of the experiment, the eelgrass was acclimated to saturating irradiance for 12 hours in the experimental tanks with flow-through seawater.

LAI treatments were created by first subsampling 100 of 300 shoots collected from Padilla Bay to estimate the average LAI of an individual shoot from this site. Then, shoot densities were chosen (0, 0, 3, 6, 9, 17, 22, 28 to obtain LAI values of approximately 0, 0, 0.5, 1.0, 1.5, 2.0, 3.0, relative to the bottom area of each tank (0.082 m^2). We had an additional 2 tanks in the 800 μatm pCO_2 treatment (see below) containing densities of 34 and 37 to obtain LAI values of 4.0 and 5.0 because we wanted to assess thresholds of carbon uptake due to self-shading Eelgrass shoots were attached by the rhizome to negatively buoyant mesh frames to position them in the tank and grown hydroponically to isolate the impact of sediment biota on carbonate chemistry. Because not all eelgrass shoots were identical, at the end of the experiment, we quantified the LAI of the eelgrass in each tank. Measured rather than target LAI was used as a continuous variable was used in analysis of results.

Light Treatments: Six grow-light fixtures (Platinum LED p600) were mounted above the experimental tanks, and each tank was randomly assigned a saturating, sub-saturating, and dark treatment. The light fixtures emitted a complete 12-band spectrum of light, from ultraviolet to upper infrared light at an intensity of 9.16 ± 0.43 mols m^{-2} d^{-1} (PAR) measured at the water surface of the tanks, which is considered saturating for eelgrass (Thom, 2008). Opaque boxes and mesh covers made from a single layer of window screen were used to cover the tanks to achieve the 'dark' and 'sub-saturating' treatments, respectively. The single layer of window screen was determined to reduce light by approximately 66%, which reaches limiting irradiance levels for eelgrass (Thom, 2008). The 'saturating' irradiance treatment were left uncovered so each tank could receive full light. Photosynthetically active radiation (PAR) was measured at the end of the incubation period using a QSL-100 irradiance sensor (Biospherical Instruments Inc.) placed 5 cm below the surface of each tank and measured under 5 cm of seawater.

Manipulation of pCO_2: To test the effect of elevated pCO_2 on the ability of eelgrass to alter carbonate chemistry, two pCO_2 treatments (800 μatm and 1800 μatm) were applied to the mesocosm system. We built a CO_2 delivery system based on methods of Jokiel et al. (2014) to manipulate pCO_2. Eight experimental tanks were enriched with CO_2 through a continuous supply of CO_2 gas regulated by a peristaltic pump (EW-07522-20 Masterflex L/S Digital Drive) (Figure 4). The CO_2 gas was delivered into the intake of a powerhead pump (Marineland Maxi-jet 900) in each tank. The magnetically-driven impeller in each powerhead pump created turbulence and cavitation around the impeller breaking the CO_2 gas into miniscule bubbles, resulting in complete dissolution of the gas into the water as it passed through the pump (Jokiel et al. 2014). An increase in pCO_2 of approximately 1000 μatm was achieved by setting the peristaltic pump to deliver 19 mL min^{-1} of CO_2 gas at 16 psi paired with water flow into and out of the tank at 3.5 L min^{-1}. The number of tank replicates for the enriched pCO_2 treatment was limited by the number of channels in the peristaltic pump (n=8). For the 'ambient' treatment, 8 tanks were set up similarly, but no CO_2 was added (Figure 4). The pCO_2 treatments were randomly assigned to the tanks and the tanks assigned as enriched pCO_2 were enriched for all experimental trials.

Incubation Trials: All the tanks had a one-hour acclimation period to the given light and pCO_2 conditions with flow-through seawater, followed by one hour incubation, during which seawater flow and CO_2 delivery was turned off and tanks were capped, creating closed systems. The incoming seawater line was transferred from the experimental tank and into an outer tank creating a circulating water jacket around each tank to maintain ambient seawater temperature throughout the experiment. Recirculating pumps continually circulated the seawater (870 L hr^{-1}) in each closed tank to promote diffusion across leaf surface-water interfaces. Each tank, with its assigned pCO_2 treatment was randomly assigned a LAI and light treatment during 3 daytime trials resulting in three replicate

measurements for each 18 LAI, light, and pCO_2 treatment combinations. Due to variability observed in the dark irradiance treatment (likely due to light leaks from imperfect shade boxes), a fourth trial was conducted after sunset, in which all tanks were incubated for 9 hours in the dark.

Measuring Seawater Chemistry: We tracked changes in water chemistry by sampling the water in each tank at the beginning and end of each incubation period. Water samples were taken from tubing placed in a small opening of the tank using a syringe to minimize gas exchange before and during sampling. We discarded the first 30 mL to rinse the tubing, drew a fresh syringe, and dispensed 60 mL of seawater into a graduated cylinder. For each tank, in situ pH_{NBS} (National Bureau of Standards), DO, and water temperature measurements were taken immediately after the sample was dispensed into the graduated cylinder. We measured pH_{NBS} and water temperature using a Thermo Scientific A221 pH_{NBS} probe and dissolved oxygen using an Orion RDO dissolved oxygen probe. The pH_{NBS} probe was calibrated using Orion pH buffer packs (pH 4, 7, and 10). The DO probe was calibrated by equilibrating the probe to the oxygen saturation in air in the calibration sleeve. We used pH_{NBS} probe measurements for real time monitoring of pCO_2 treatments and used the total scale pH (pH_t) for modelling calculations (see below).

Discrete water samples for nutrients, dissolved TCO_2 and pH_t were also taken at the beginning and end of each trial. Samples for nutrients were syringe filtered using a glass fiber filter, and frozen until analysis. Nitrate plus nitrite measurements were based on the Griess diazotization reaction and were conducted with a Lachat QuikChem 8500 autoanalyzer (method #: 31-107-04-1-G). Phosphate was analyzed with the ascorbic acid method also on the Lachat QuikChem 8500 autoanalyzer (method #: 31-115-01-1-H). Two carbonate samples were collected by drawing two unfiltered 30-ml syringes to fill duplicate 20 mL scintillation vials bottom-up and overflowing the vial. Ten µl of saturated

$HgCl_2$ was added to each sample to eliminate any biological activity, and the samples were refrigerated at 10°C for two weeks before analysis for dissolved TCO_2 and pH_t.

Both pH_t and TCO_2 were measured on each sample. The vials were placed in a water bath at 25 °C for 40 minutes and then analyzed consecutively for pH_t using a spectrometer (Ocean optics Flame-S-UV-VIS) and for TCO_2 with a dissolved inorganic carbon analyzer (Apollo SciTech AS-C3, Cai and Wang 1998). Water temperatures were monitored using a Fluke 1523 reference thermometer and probe. We measured pH_t using a modification of the m-cresol method (Clayton and Byrne 1993, Dickson et al. 2007). To analyze a sample, a 5-cm water jacketed cuvette was rinsed with DI water, then rinsed with part of the sample, and then overflowed with the sample using a syringe. After a baseline spectrum was taken, 30 μL of m-cresol dye was added, and a second spectrum collected. The remaining sample not used in the pH_t measurement was used concurrently for dissolved inorganic carbon (DIC) analysis. The instrument acidified the sample with 10% phosphoric acid to convert all carbonate species to CO_2, then nitrogen gas was bubbled through the seawater so that TCO_2 could be quantified using a gas phase infrared CO_2 detector. TCO_2 was analyzed by measuring two 0.75 mL subsamples.

Initial and final TCO_2 and pH_t measurements were used to calculate the associated carbonate chemistry parameters, including the change in aragonite saturation state (Ω_{Ar}) and the change in the partial pressure of CO_2 (pCO_2) using CO_2SYS (Pierrot et al. 2006) with K_1 and K_2 equilibrium constants from Mehrbach et al. (1973) and refit as in Dickson and Millero (1987). Differences in water chemistry were calculated by subtracting the initial from the final values for TCO_2, pH_t Ω_{Ar} pCO_2, and dissolved oxygen (DO). Differences were corrected for non-eelgrass effects by

subtracting the observed mean difference in the blank tanks from the observed differences in each eelgrass tank.

Eelgrass tissue measurements: Because few studies have used LAI as a metric for eelgrass abundance in relation to carbon uptake, we collected additional eelgrass metrics that we could use for comparison to existing studies. All eelgrass biomass in each tank was collected immediately after the incubations and quantifying LAI, separated at the meristem into above- and below-ground tissues and dried at 60°C for at least 24 hours (Fisher Scientific Isotemp 500 series) following the methods outlined by Short and Duarte (2001). Dry weights of eelgrass for each tank were measured using a Mettler Toledo XS205 scale.

Eelgrass leaf chlorophyll content was determined following the methods outlined by Dennison (1990). Leaf clippings (two cm long) were taken from the middle section of the 2nd youngest leaf and then split in half. One half was ground using a micropestle tip on a power drill for 2 minutes in 2 mL of 90% acetone and the other half was dried for biomass. Once the leaf tissues were ground up, the chlorophyll was extracted in 5 mL of 90% acetone in the dark at 4 °C for 24 hours. Then, chlorophyll samples were centrifuged for 10 min at 5000 rpm to get rid of the leaf tissue. Once the chlorophyll was extracted and leaf tissues were separated, we measured the fluorescence absorbance of 1 mL samples using a fluorometer (Turner Designs, Trilogy fluorometer). Chlorophyll content was calculated using the equations described by Inskeep and Bloom (1985) and normalized to dry biomass (mg).

Statistical Analyses

Field Data: To assess leaf area index (LAI) differences between sites across Washington State and to identify differences in LAI between elevations in Padilla Bay, WA, we used separate 1-way analyses of variance for each variable. Assumptions of normality and homogeneous variance were assessed using Shapiro-Wilk and Levene's tests respectively. To identify which LAI values were different, we used orthogonal contrasts to compare high LAI values (LAI >3) to low LAI values (LAI <3).

Experimental Data: Since the dark treatments in the initial 3 day-time trials were not completely dark (Figure A1), they were analyzed separately from the sub-saturating and saturating light data. The overnight trial had only 1 light condition (dark), and was also analyzed separately. For the day-time trials (sub-saturating and saturating light data only), we used model selection to determine which factors (LAI, pCO_2 and irradiance) best predicted changes in carbonate chemistry. We used a top-down process for model selection and started with a beyond optimal model where the fixed component of the model included all explanatory variables (LAI, pCO_2, irradiance, change in water temperature, nitrate and nitrite concentration, and phosphorus concentration). We determined the optimal structure of the random components (tank and experimental trials) by comparing nested models using residual maximum likelihood estimation. We assessed all factors (random, covariate and fixed factors) using the likelihood ratio test where higher values indicated a better "goodness of fit" and using Akaike information criterion (AIC) values where lower AIC values indicate higher quality models. Once the best random structure was found, we determined the optimal fixed structure by comparing nested fixed effects using maximum likelihood estimation also using AIC values. The model variance structure was validated by comparing residuals with fitted values to identify violation of homogeneity, indicated by differences in spread.

We assessed eelgrass self-shade effects at higher LAI values by fitting different models; a linear and a quadratic model. We assessed which model best predicted changes in ΔTCO_2 using a Chi-square test to compare the AIC values. Normality and homogeneous variance were assessed by comparing residuals against fitted values.

We normalized ΔTCO_2 to chlorophyll to assess differences between pCO_2 levels using an analysis of variance test. Normality and homogeneous variance were assessed using a Shapiro-Wilk and Levene's tests respectively. We used orthogonal contrasts to identify differences in ΔTCO_2 per chlorophyll for each pCO_2 level.

Modeling: Effects of Residence Time & Depth

To understand how our rates of carbon uptake translate to eelgrass meadows in the field, we calculated differences in how our measured rate of carbon uptake would influence water chemistry for a range of water depths and residence times. We used the 'AICcmodavg' package in R to calculate the predicted mean and standard error in the change in rate of TCO_2 based on different combinations of the treatments (LAI, Light, and pCO_2). The rates of pCO_2 increase were calculated for LAI values of 1, 3, and 5 and for the ambient (800 μatm) and enriched (1800 μatm) pCO_2 treatments at saturating light. Changes in pCO_2 were calculated based on the change in rates of total carbon uptake from the mean of each pCO_2 treatment level (800 μatm and 1800 μatm) but assumed no change in alkalinity using CO_2SYS. The standard error for the change in TCO_2 was also calculated by subtracting the standard error from each pCO_2 treatment level mean. All statistical analyses were conducted using R (R Core Team 2016).

Results

Field Surveys for Leaf Area Index (LAI)

Our field data demonstrated leaf area index (LAI) differences between sites and with elevation within a single site (Figure 5). The mean LAI by site (± standard error) ranged from 0.86 ± 0.11 LAI to 3.35 ± 0.28 LAI at an elevation of -1 m relative to MLLW. The LAI in Washington state (Figure 5A) and at Padilla Bay, WA (Figure 5B) were normally distributed (Table A1) and the variance was homogenous (Table A2). We found site differences throughout Washington (Table A3) where the LAI at Nisqually Reach, Willapa Bay, and Skokomish was greater than the LAI at Fidalgo Bay, Case Inlet, and Port Gamble (Figure 5A, Table A4). At Padilla Bay, we found a difference in LAI across elevations (Table A3) where elevations between -1 and -2.0 m had greater LAI than at locations sampled between +1 and -1 m depths (Figure 5B, Table A4). The range of LAI values observed in the field (0 to 7 LAI) spans the same range as the LAI used in the mesocosm experiment (0-4.8 ambient, 0-3.8 enriched). The above and belowground biomass of the maximum LAI value (4.7 LAI) were 220.1 g dry wt m^{-2} and 131.7 g dry wt m^{-2} respectively. The densities, aboveground biomass, and below ground biomass for the field and the experiment can be found in Figure A2.

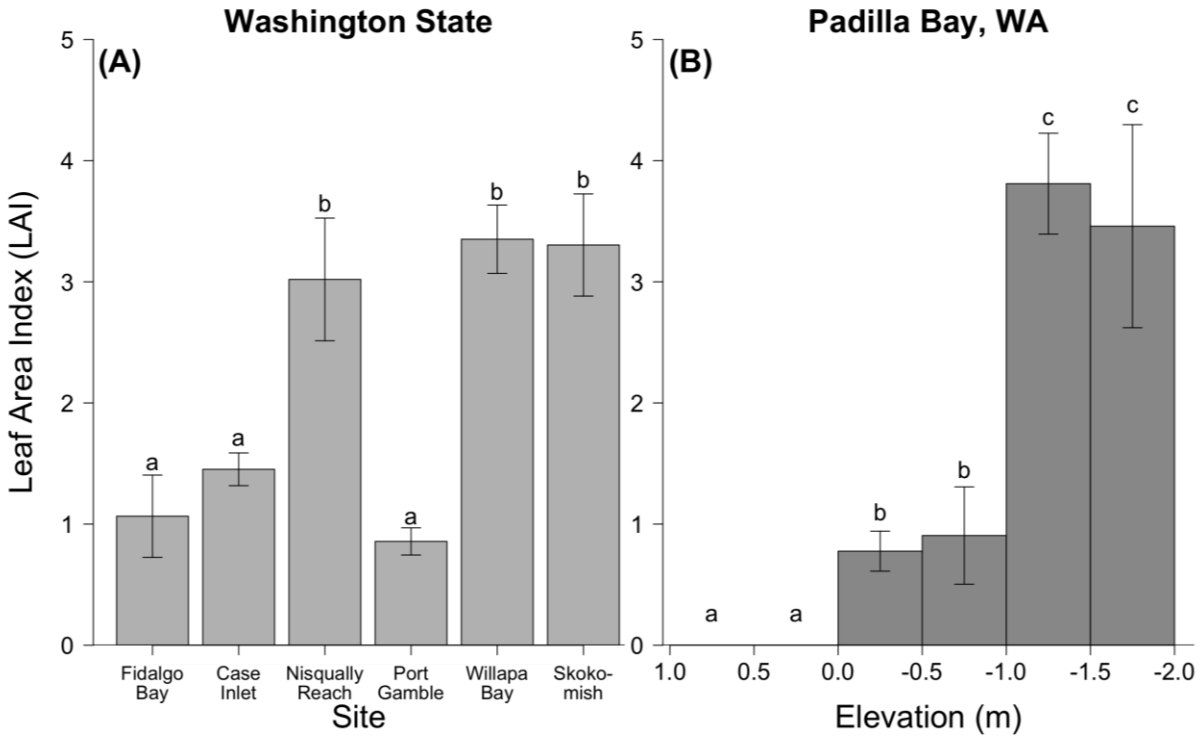

Figure 5. (A) Leaf area index (LAI) field survey of Washington State – LAI (total leaf area/total ground area) of *Zostera marina* was sampled at Fidalgo Bay, Case Inlet, Nisqually Reach, Port Gamble, Skokomish, and Willapa Bay, WA (N= 12, 9, 9, 9, 9, and 9 respectively). LAI measurements were sampled at -1m depths and at 5, 10 and 15m along 3 transects at each site except Fidalgo Bay, which was sampled at 8 distances across one transect. (B) LAI of *Zostera marina* at Padilla Bay, WA was sampled across at elevations (m) ranging from 1 to -2m. Each elevation range was sampled 3 times across 3 separate transects placed perpendicularly to shore. The error bar are the 95% confidence intervals and the letters represent LAI differences across sites (A) and tidal elevations (B) based on the results of orthogonal contrasts.

Effects of LAI, pCO_2 and Irradiance on ΔTCO_2

We calculated ΔTCO_2 with adjustment for the mean differences in control tanks (LAI= 0) and applied this correction to all tanks since it did not affect the outcome of the model except for the intercept term (Table A5, Figure A3). Based on the output of the most parsimonious model after model selection (Table 1), ΔTCO_2 was affected by the interaction of LAI and light and the interaction of LAI, light, and pCO_2 (Figure 6, Table 2), or any other covariate effects (Table 1). We found that eelgrass in saturating light took up carbon at an increasing rate as LAI increased (Figure 6, Table 2). The rate of carbon uptake per unit LAI was even greater when eelgrass was exposed to enriched pCO_2 (1800 μatm) (Figure 6, Table 2). This model estimated a decrease in ΔTCO_2 of 7.128 μmol TCO_2 kg^{-1} Hr^{-1} per unit LAI at 800 μatm pCO_2 treatment and at saturating light (Figure 6, Table 2). However, under enriched pCO_2 (1800 μatm) and saturating light, the estimated ΔTCO_2 decreased an additional 7.304 μmol TCO_2 kg^{-1} Hr^{-1} per unit LAI (Figure 6, Table 2). At the maximum LAI value (LAI=4) under saturating light conditions, rates of carbon uptake were 34.5 ± 3.4 and 54.4 ± 5.3 μmol kg^{-1} Hr^{-1} for the 800 μatm and 1800 μatm pCO_2 treatments respectively (Figure 6). However, when ΔTCO_2 was normalized to the amount of chlorophyll per tank we found no discernable differences between pCO_2 treatments (Table A6). There was still an interaction between LAI and light in the ΔTCO_2 normalized data (Table A6). Overall, the maximum rate of carbon uptake of eelgrass was 131 ± 12 (SE) μmol TCO_2 mg chl^{-1} hr^{-1} (N=54, Figure A4). At sub-saturating light conditions the rate of carbon uptake of eelgrass was not affected by LAI or enrichment of pCO_2 (Figure 6, Table 2).

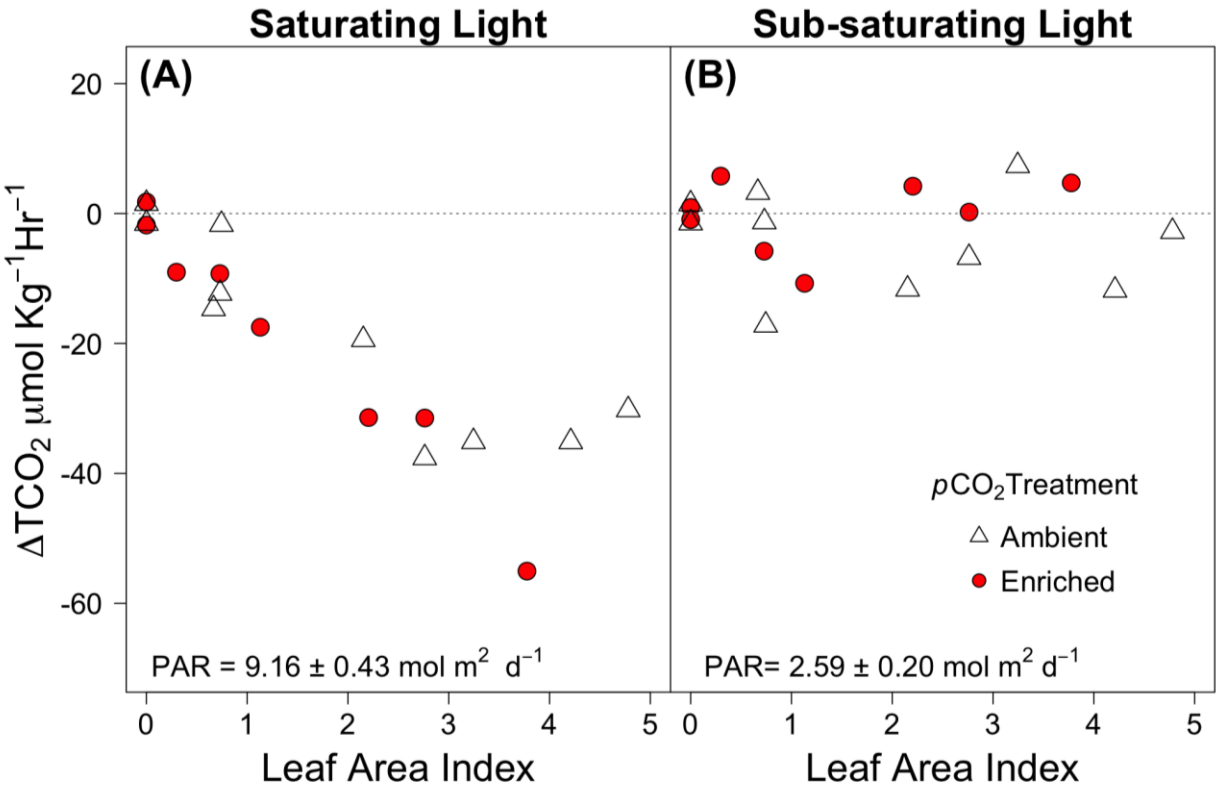

Figure 6. Change in the rate of change in carbon uptake (ΔTCO_2 µmol kg^{-1} Hr^{-1}) compared to the LAI of eelgrass ranging from 0 to 5 for (A) saturating and (B) sub-saturating light levels (left and right panels). The response was calculated by subtracting the final TCO_2 measurements from the initial TCO_2 measurements (over the one hour incubation period). Open triangles represent ambient pCO_2 (800 µatm) and red circles represent enriched pCO_2 (1800 µatm). The mean differences in control tanks (LAI= 0) were adjusted to zero and this correction was applied to all tanks where the difference was +4.368 and -11.679 µmol kg^{-1} Hr^{-1} for the ambient pCO_2 response (800 µatm) and -1.395 and -14.520 µmol kg^{-1} Hr^{-1} (N=10) for the enriched pCO_2 response (1800 µatm, N=8) for saturating and sub-saturating light levels respectively. Average photosynthetic active radiation (PAR) ± standard error (N=18) are reported at the bottom of each figure. The experimental model estimates that the rate of change in carbon uptake (ΔTCO_2 µmol kg^{-1} Hr^{-1}) = -3.003 –0.564(LAI) +1.29(CO_2) –0.777(Light), +1.67(LAI*CO_2) -7.128(LAI*Light) +1.432(CO_2*Light) -7.304(LAI*CO_2*Light) where LAI is equal to the tested LAI value, CO_2 is equal to 1 if enriched, and LAI is equal to 1 if saturating.

Table 1. Comparison of models using the top-down approach and the likelihood-ratio test to determine the most parsimonious model to predict ΔTCO_2. We assessed the random variance structure (experimental trial and tank) using a linear mixed-effects model (lme) and the residual maximum likelihood estimation method (REML). Covariate effects (change in water temperature, ΔTemp.) were assessed using the generalized linear squares model (gls) and the maximum likelihood estimation method (ML). These analyses were conducted separate from the dark data of the over-night experimental trial where model, estimation method, degrees of freedom (*df*), Akaike information criterion (AIC), log likelihood (logLik), model test, liklihood ratio (L Ratio) and the respective *p*-values are reported below. The full fixed effects model included all possible interactions between fixed effects ($\Delta TCO_2 \sim LAI + CO_2 + Light + LAI{:}CO_2 + LAI{:}Light + CO_2{:}Light + LAI{:}CO_2{:}Light$).

Model	**Estimation**	***df***	**AIC**	**logLik**	**Test**	**L Ratio**	***p*-value**
lme1 (full fixed effects model + Trial + Tank)	REML	16	225.5	-96.7			
lme2 (full fixed effects model + Tank)	REML	13	226.2	-100.1	lme1 vs lme2	6.75	0.081
lme3 (full fixed effects model + Trial)	REML	13	221.5	-97.1	lme1 vs lme3	2.00	0.573
gls1 (full fixed effects model)	REML	10	220.2	-100.1	lme3 vs gls1	6.75	0.344
gls1 ($LAI + CO_2 + Light + LAI{:}CO_2 + LAI{:}Light + CO_2{:}Light + LAI{:}CO_2{:}Light + \Delta Temp$)	ML	10	248.5	-114.3			
gls2 ($LAI + CO_2 + Light + LAI{:}CO_2 + LAI{:}Light + CO_2{:}Light + LAI{:}CO_2{:}Light$)	**ML**	**9**	**248.0**	**-115**	**gls1 vs gls2**	**1.42**	**0.233**

Table 2. Generalized least squares model summary – gls2 (normalized ΔTCO_2~LAI*CO_2*Light) including the factor, estimate, standard error (SE), t-value, *p*-value using the maximum likelihood estimation and excluding the dark data from the over-night experimental trial. The residual standard error was 5.899 and the model had 36 degrees of freedom. These data were analyzed by subtracting the mean of the control tanks (LAI= 0) from tanks containing eelgrass. The mean ΔTCO_2 of the controls for the saturating and sub-saturating light levels were -4.37 and -11.68 μmol TCO_2 kg^{-1} Hr^{-1} for the ambient pCO_2 treatment (800 μatm) and 1.40, and -14.52 for the enriched pCO_2 treatment (1800 μatm). Significant factors (*p*-value < 0.05) are in bold.

Factor	**Estimate**	**SE**	**t-value**	***p*-value**
(Intercept)	-3.003	3.239	-0.93	0.361
LAI	-0.564	1.271	-0.44	0.661
CO_2 (Enriched)	1.29	4.701	0.27	0.786
Light (Saturating)	-0.777	4.58	-0.17	0.867
LAI:CO_2 (Enriched)	1.67	2.205	0.76	0.455
LAI:Light (Saturating)	**-7.128**	**1.798**	**-3.96**	**<0.001**
CO_2 (Enriched):Light (Saturating)	1.432	6.649	0.22	0.831
LAI: CO_2 (Enriched):Light (Saturating)	**-7.304**	**3.118**	**-2.34**	**0.027**

Functional Relationship between LAI and ΔTCO_2 in ambient pCO_2 conditions:

A quadratic relationship best fit the rates of carbon uptake with LAI, in saturating light conditions at ambient pCO_2 conditions (800 μatm) (Figure 7, Table A7, Table A8). A quadratic model explained more of the variance in ΔTCO_2 than a linear model indicated by a lower AIC value and higher logliklihood ratio (Table A7). For the enriched pCO_2 treatment (1800 μatm), the linear model best fit ΔTCO_2 since a linear model was not different than the quadratic (Table A7). Using the quadratic model fit for the ambient pCO_2 treatment, the maximum rate of carbon uptake occurred at an LAI of 3.96 and was approximately -38.4 μmol TCO_2 kg^{-1} Hr^{-1} (Figure 7, Table A8).

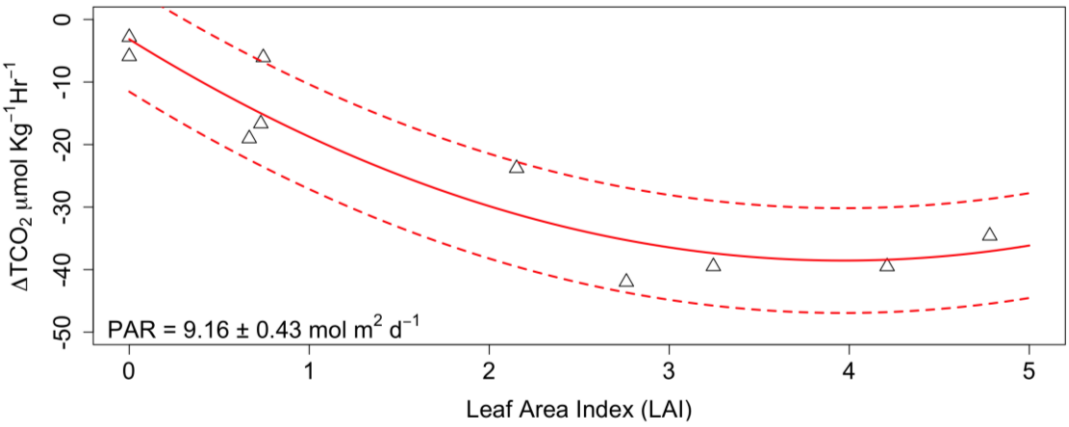

Figure 7. Change in the total carbon uptake (ΔTCO_2 μmol kg^{-1} Hr^{-1}) for ambient pCO_2 data (800 μatm) compared to the LAI of eelgrass ranging from 0 to 5 for saturating light. The mean differences in control tanks (LAI= 0) were adjusted to zero and this correction was applied to all tanks where the difference was +4.368 μmol kg^{-1} Hr^{-1} for the ambient pCO_2 response (N=10). A quadratic function was used to model the response. Average photosynthetically active radiation (PAR) ± standard error (N=18). The equation for the curve is the change in TCO_2 (ΔTCO_2 μmol kg^{-1} Hr^{-1} = $2.25(LAI)^2$ - 17.84(LAI) - 3.16.

Saturating Light Data – pH, Ω_{Ar}, and pCO_2

Other parameters, such as pH and calculated Ω_{Ar} and pCO_2 also changed based on the interactive effects of LAI and Light (Figure 8). Under saturating light conditions, pH, Ω_{Ar}, and pCO_2 were not affected by the random effects (experimental trial and tank) or covariate effects (changes in water temperature) (Table A9). We did not observe any effects of pCO_2 treatment on changes in pH, Ω_{Ar}, and pCO_2 (Table A10). However, our experimental models indicate that at saturating light, the magnitude of ΔpH, $\Delta\Omega_{Ar}$ and ΔpCO_2 (μatm Hr^{-1}) increase with increasing LAI (Figure 8, Table A10). The rate of change for pH, Ω_{Ar}, and pCO_2 based on our experiment was 0.05 (±0.01) pH units Hr^{-1}, 0.11 (±0.04) Ω_{Ar} Hr^{-1}, and -87 (±19.6) μatm Hr^{-1} for every unit increase in LAI under saturating light conditions (Figure 8, Table A10). At the maximum LAI (LAI=4), these rates of change correspond to a pH increase of ~0.2 (±0.04) pH units Hr^{-1}, aragonite saturation state increase of ~0.45 (±0.12) Ω_{Ar} Hr^{-1}, and a pCO_2 decrease of 348 (78.4) μatm Hr^{-1} (Figure 8, Table A10).

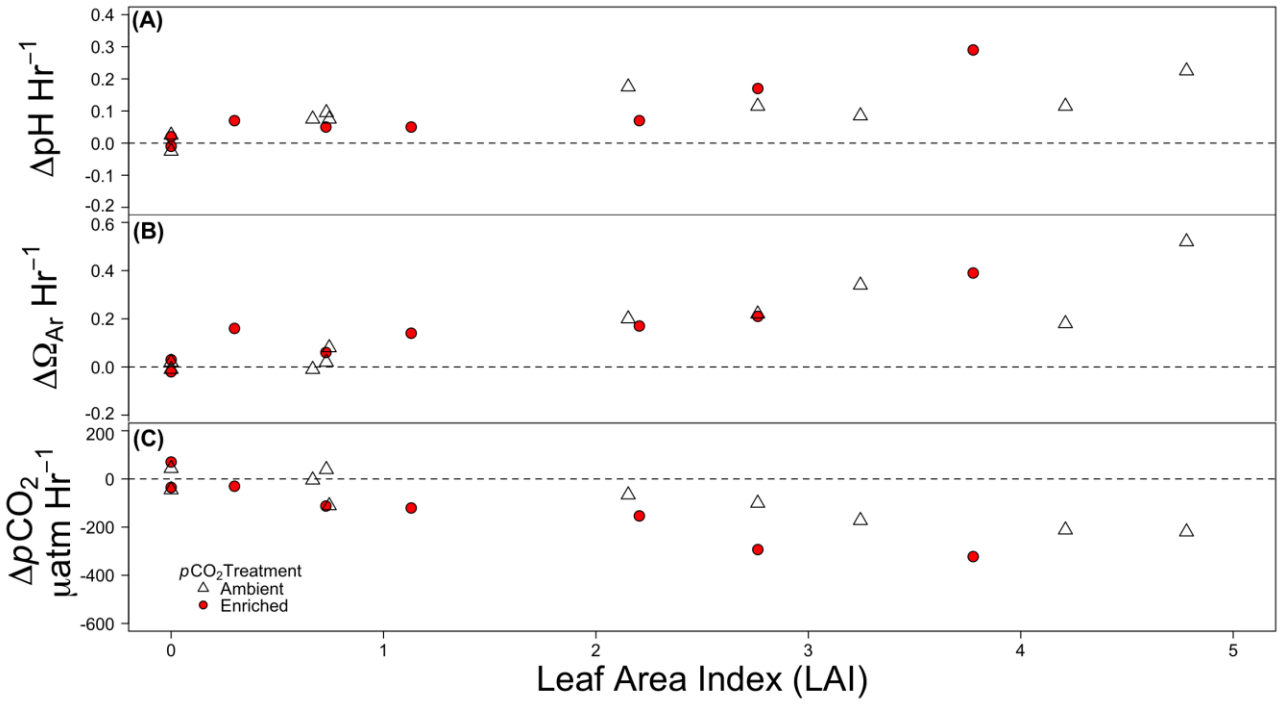

Figure 8. The changes in pH (ΔpH Hr^{-1}), Ω_{Ar} ($\Delta\Omega_{Ar}$ Hr^{-1}), partial pressure of CO_2 (ΔpCO_2 µatm Hr^{-1}). These response variables are shown across leaf area index (LAI) values and between ambient pCO_2 (800 µatm) in open triangles and enriched (1800 µatm) pCO_2 in red circles.

Dark Data – Effects of LAI on TCO_2, pH, Ω_{Ar}, and pCO_2

In the night-time experimental trial, pCO_2 treatments did not affect TCO_2, pH, Ω_{Ar}, or pCO_2 (Figure 9, Table A11). Therefore, these data were analyzed using a linear model of the response as a function of leaf area index (Table A10, Table A12). We found that for every unit increase in LAI, the rate of carbon release was 0.86 ± 0.23 µmol TCO_2 kg^{-1} Hr^{-1} and decreased pH by 0.003 ± 0.001 pH units Hr^{-1}, decreased Ω_{Ar} by 0.004 ± 0.003 Ω_{Ar} Hr^{-1}, and increased pCO_2 by 8.4 ± 3.4 µatm Hr^{-1} (Figure 9, Table A12). At the maximum LAI (LAI=4), these rates of change correspond to a TCO_2 increase of 3.44 ± 0.92 µmol TCO_2 kg^{-1} Hr^{-1}, a pH decrease of 0.012 ± 0.004 pH units Hr^{-1}, a Ω_{Ar} decrease of ~0.016 ± 0.012 Ω_{Ar} Hr^{-1}, and a pCO_2 increase by 33.6 ± 13.6 µatm Hr^{-1}. Overall, the rate of carbon increase of eelgrass in the dark was approximately 10.7x less than the rates of carbon decrease when in saturating light (Figure 8, Figure 9, Table A12).

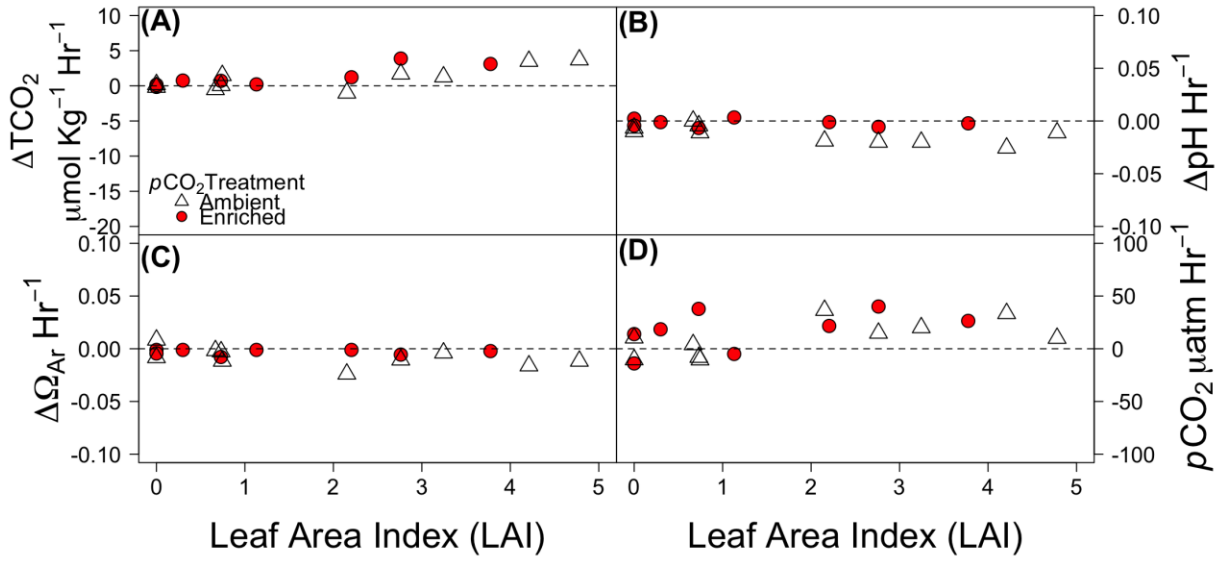

Figure 9. The night-time experimental trial in the dark showing (A) the rate of change in TCO_2 (ΔTCO_2 μmol kg^{-1} Hr^{-1}), (B) the rate of change in pH (ΔpH Hr^{-1}), (C) the rate of change in aragonite saturation state (Ω_{Ar} Hr^{-1}), and (D) the rate of change in partial pressure of CO_2 (ΔpCO_2 μatm Hr^{-1}). Each response variable is shown across LAI treatments where the red circles and black triangles represent the enriched (1800 μatm) and ambient (800 μatm) pCO_2 treatments respectively.

Water Depth and Residence Time

In the real world, water depth in eelgrass meadows is variable and increased water volume results in smaller changes in water chemistry due to carbon uptake despite high LAI values and saturating light conditions (Figure 10). Even though rates of carbon uptake and changes in other parameters in this study were substantial at saturating light conditions, high LAI, and enriched pCO_2 conditions (1800 μatm), those results were achieved with a relatively small volume of water and a long residence time. Small increases in depth can diminish changes in ambient TCO_2, pH, and saturation state by essentially diluting the effect of the eelgrass in a larger volume of water (Figure 10). For example, even at only 1 meter depth, the change in CO_2 per hour is less than half what it was at 40 cm and only in the enriched pCO_2 treatment does even the highest LAI produced changes of more than 100 μatm Hr^{-1} in 1 meters of water (with a one hour residence time) (Figure 10).

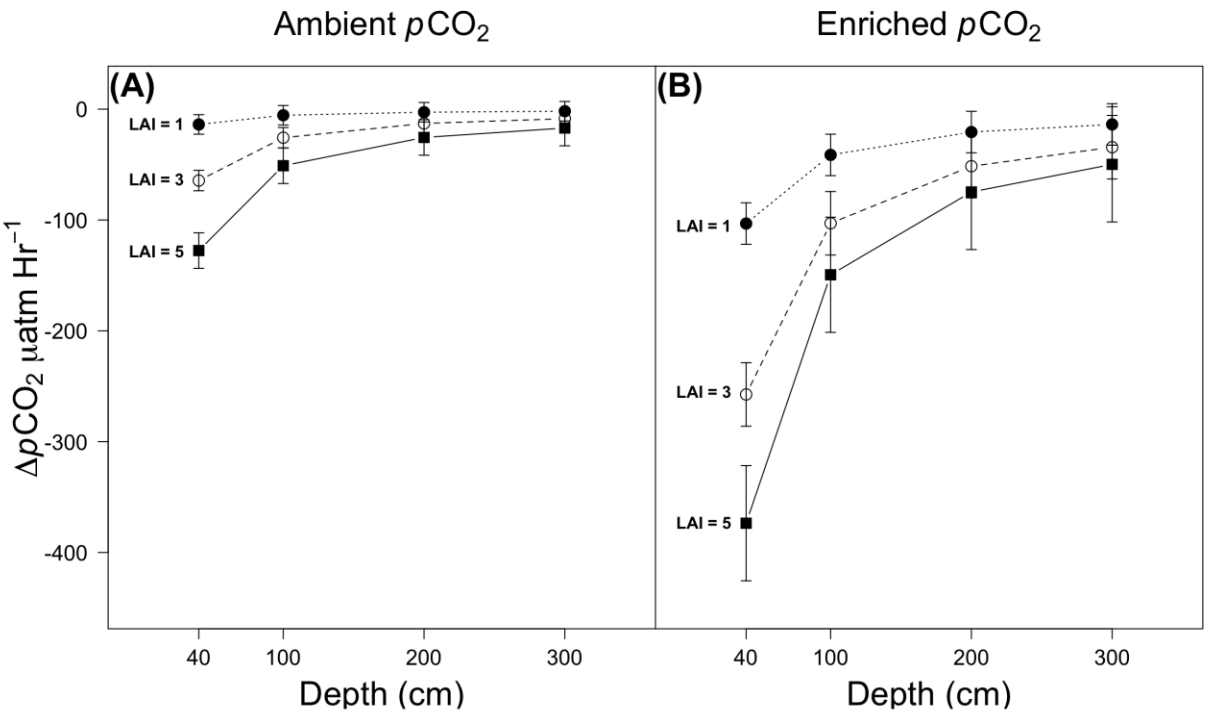

Figure 10. Changes in the partial pressure of CO_2 (ΔpCO_2 µatm Hr^{-1}) across different water depths (cm). The black circles with dotted lines, open circles with dashed lines, and black squares with a solid line represents LAI values of 1, 3, and 5 respectively for the ambient pCO_2 treatment (800 µatm) on the left panel (A) and the enriched pCO_2 treatment (1800 µatm) on the right panel (B). The estimations for pCO_2 across depth were calculated in CO_2SYS based on rates derived from the experimental model for TCO_2. Error bars represent 95% confidence intervals.

Additionally, shorter residence time can further decrease the ability of even high LAI treatments under saturating light conditions to change the ambient water chemistry (Figure 11). For the ambient pCO_2 treatment (800 µatm), the highest LAI produced changes of more than 100 µatm Hr^{-1} only when residence times were 50 min or greater (Figure 11A). Whereas, in the enriched pCO_2 treatment (1800 µatm), the highest LAI produced changes of more than 100 µatm Hr^{-1} when residence times were 20 minor greater (Figure 11B). Therefore, the enriched pCO_2 treatment resulted in similar amounts of pCO_2 increase at shorter residence times than the ambient pCO_2 treatment. However, the rate of pCO_2 increase will diminish despite the effect of pCO_2 enrichment and high LAI with shorter residence times.

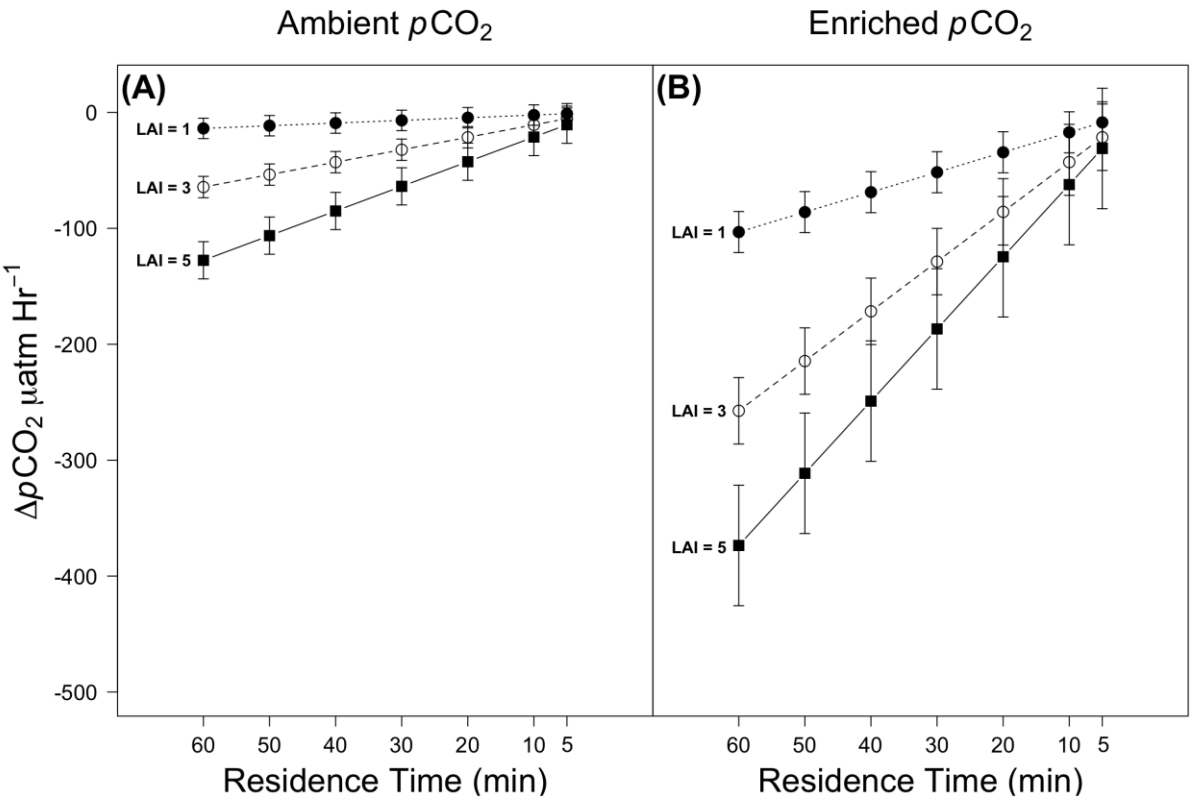

Figure 11. Changes in the partial pressure of CO_2 (ΔpCO_2 µatm Hr^{-1}) across different residence times (min). The black circles with dotted lines, open circles with dashed lines, and black squares with a solid line represents LAI values of 1, 3, and 5 respectively for the ambient pCO_2 treatment (800 µatm) on the left panel (A) and the enriched pCO_2 treatment (1800 µatm) on the right panel (B). The estimations for pCO_2 across depth were calculated in CO_2SYS based on rates derived from the experimental model for TCO_2. Error bars represent 95% confidence intervals.

Discussion

The focus of this study was to assess the potential of eelgrass meadows to take up carbon within the context of realistic ranges of eelgrass leaf area index (LAI) values, pCO_2, and light, like those observed in the Salish Sea (Figure 5, Figure 6, Table A13). We compared rates of carbon uptake between LAI, pCO_2, and light treatments to better understand how these factors interact to modify the variability of acidification to help natural resource managers estimate the effects of eelgrass carbon uptake on localized water chemistry in different sites throughout the Salish Sea.

Influence of Leaf Area Index (LAI)

The ability of eelgrass meadows to measurably take up carbon depends on the amount of photosynthetic leaf area per ground area which changes between sites and between elevations. When there was more eelgrass leaf area per ground area, or higher leaf area index (LAI) values, rates of carbon uptake increased under saturating light for both pCO_2 conditions, resulting in marked changes in carbonate chemistry under the conditions tested here especially for tanks with LAI value near 4 (Figure 6). However, LAI values vary between sites and our field surveys demonstrate that not all eelgrass sites nor all locations within these sites have sufficient LAI values to take up enough carbon to make a measureable difference in ambient water chemistry (Figure 5, Table A3). We observed generally increasing LAI with increasing depth at Padilla Bay where lower LAI values occurred at the higher intertidal areas (Figure 5B). The elevation and LAI relationship suggests that eelgrass meadows at deeper locations throughout the Salish Sea are likely to have greater LAI and are therefore more likely to take up carbon at a higher rate (Figure 5B, Table A3, Figure A2). However, even at a single elevation of -1 m, there is considerable variation the LAI by site (Figure 5B, Table A3), indicating that depth alone is not a sufficient predictor of meadow capacity for

carbon uptake. Additionally, increasing LAI with depth is balanced by potentially lower light conditions as depth increases (Dennison and Alberte 1985, Dennison 1987). In 50 to 100 years at high latitudes, water depth is expected to increase by 0.5 m (Trenberth 1996) and could cause shifts in the location and density of eelgrass beds (Backman and Barilotti 1976, Duarte 1991, Short et al. 1993, Short et al. 1995).

Meadow size and shape can also affect shoot densities and abundance since eelgrass meadows located at fringe sites (common in central Puget Sound and Hood Canal) tend to have meadows that are smaller in area than eelgrass meadows located at tidal flats such as Padilla Bay, Fidalgo Bay, and Birch Bay (Christaen et al. 2016). Eelgrass meadows throughout the Salish Sea exhibit large differences in shoot length, sheath width, and abundance of the eelgrass (Figure A2) which could affect photosynthetic rates of eelgrass and responses to changes in light and pCO_2 levels. The use of LAI makes sites with different morphologies and abundances more comparable but cannot eliminate these effects all together.

Our field survey highlighted these aboveground biomass and abundance differences between sites (Figure A2). Sites such as Case Inlet and Port Gamble had more abundant eelgrass but the LAI values and the aboveground biomass was much lower than sites at Nisqually Reach, Willapa Bay, and Skokomish where LAI was greatest and eelgrass was less abundant (Figure A2). Therefore, assessing the photosynthetic capacity of an eelgrass meadows based on abundance of eelgrass may not be a good indicator compared to LAI and above ground biomass.

Self-shading effects at higher LAI

Interestingly, we observed reduced photosynthetic rates at higher LAI values for the ambient pCO_2 data (800 μatm) most likely due to self-shading effects or co-limitation of carbon and light (H_1, Figure 7, Table A8). This is demonstrated by the fact that the relationship between the rate of carbon uptake and LAI for the ambient pCO_2 data (800 μatm) was best described using a quadratic equation with a carbon uptake maximum at a LAI of 3.96 (Figure 7, Table A8). Our field observations of LAI values support this quadratic relationship since the mean LAI values at all sites were below 3.96 indicating that natural meadows may be at carrying capacity due to growth limitation near this same threshold (Figure 5). For the enriched pCO_2 data (1800 μatm), we did not observe reduced carbon uptake instead, ΔTCO_2 was linear with increasing LAI (Figure 7, Table A7, Table A8). However, the maximum LAI for the enriched pCO_2 treatment was only 3.8, which may not be high enough for self-shading effects to emerge (Figure 7, Table A7, Table A8). It is possible that eelgrass in the enriched pCO_2 treatment could reach higher LAI before carbon uptake levels off since eelgrass can directly take up CO_2 (Beer and Rehnberg 1997). Whereas, under ambient pCO_2 conditions (800 μatm) CO_2 is less available and eelgrass must produce carbonic anhydrase to dehydrate HCO_3^- to CO_2 (Beer and Rehnberg 1997). Co-limitation of light and carbon may be controlling the maximum rate of carbon uptake of eelgrass in the ambient pCO_2 treatment, but further investigation of higher LAI values is needed to determine this.

We normalized our rates of carbon uptake to chlorophyll since the chlorophyll content is an essential component of photosynthesis and allows us to compare our rate of carbon uptake to other studies. However, we found no observable thresholds in the rate of carbon uptake between pCO_2 treatments. Where if self-shading is occurring, rates should be lower per chlorophyll in tanks with the highest LAI. Our ability to detect this effect when normalizing our rates of carbon uptake to chlorophyll may be hindered by the variability of our chlorophyll measurements since they are extrapolated from a few leaf clippings to characterize the whole tank (Table A6, Figure A4). Thus, LAI is a better parameter for characterizing rates of carbon uptake in our tanks since LAI values were not extrapolated.

LAI of seagrasses

Eelgrass (*Zostera marina*) is the dominant seagrass in temperate areas and has a higher maximum LAI compared to other species of seagrasses in the tropics. For instance, summer field surveys of LAI values of *Posidonia oceanica,* meadows ranged from approximately 0 to 3.48 (Hendriks et al. 2014) whereas in the Salish Sea, LAI values of eelgrass meadows were similar though possibly slightly higher, ranging from approximately 0 to 4.7 (Figure 5). Despite differences in the range of LAI, both temperate and tropical seagrasses had similar mean LAI values where *Posidonia oceanica*, has a mean LAI of about 1.96 averaged across 14 sites throughout the west Mediterranean, Spain (Hendriks et al. 2014) and *Z. marina* in WA state has a mean LAI of 1.95 ± 0.18 (Figure 5A). Therefore, the overall photosynthetic capacity of tropical and temperate seagrasses may be similar but certain sites in temperate seagrass meadows could have a greater photosynthetic capacity since the maximum LAI is greater than at tropical seagrass meadows.

In another example, in a meadow consisting of predominantly *Thalassia testudinum* but, with *Halodule wrightii, Syringodium filiforme*, *Ruppia maritima,* and *Halophila engelmannii* also present, seagrasses reached a maximum LAI of approximately 2.5-3.0 (Hill et al., 2014). *Cymodocea rotundata,* another tropical seagrass, only reaches a maximum LAI of approximately 1.0 (Wicaksono and Hafizt, 2013). In contrast, in temperate waters, the maximum LAI value identified at Padilla Bay, Washington was approximately 4.7 for *Zostera marina* (Figure 5B). Since the localized drawdown of carbon from the waters by eelgrass photosynthesis appears to be mainly a linear function of LAI for *Zostera marina,* the greater abundance of leaf area per substrate area in this species may indicate greater potential to remove carbon from the water than some of the species with lower LAI's.

Influence of pCO_2 Enrichment

In addition to the positive effects of high LAI on rates of carbon uptake, the range of pCO_2 values tested in this study generated different rates of carbon uptake (H_2) but there are caveats to this conclusion. These findings rely on the saturating light data and sample size was small, with an unbalanced design between pCO_2 treatments (Figure 4). The enriched pCO_2 treatment (1800 μatm) only had a sample size of 8 because of the number of channels on the pump, whereas the ambient pCO_2 treatment (800 μatm) had a sample size of 10 (Figure 4, Figure 6). Thus, the ambient pCO_2 treatment contained 2 additional high-leverage data points (Altman and Krzywinski, 2016) which were at higher LAI values than the LAI values observed in the enriched pCO_2 (Figure 6). Furthermore, we couldn't detect pCO_2 treatment differences when we normalized rates of carbon uptake on a per chlorophyll basis which may be due to variability in our chlorophyll measurements (Figure A4, Table A6), but does not lend confidence to the findings of a strong effect of pCO_2 on photosynthetic rates.

Given the lack of replication and unbalanced design in our data, it is necessary that the pCO_2 treatment effect we detected be placed in context with other studies that have also investigated this question (Figure 12). Comparisons are sometimes difficult because differences in rates of carbon uptake within and between studies could be due to differences in initial TCO_2 concentration, differences in the range of TCO_2 concentrations, differences in light levels, differences in acclimation, and differences in methodology (Table 3). We have attempted to make this comparison based on change in pH (the most broadly available carbonate parameter), and change in relative photosynthetic rate. Zimmerman et al. (1997) tested pH ranges of 8.2 to 6.0 and Invers et al. (2001) tested pH ranges of 8.0 to 6.0 respectively, compared to our range of 7.76 ± 0.02 to 7.34± 0.02 pH units (Table A13). Given that the difference in photosynthetic rates increased by 290% over that range of pH (and total organic carbon) treatments in Zimmerman et al. (1997), if the increase is linear, then our change in total organic carbon is 4.5% of theirs, and the expected change in PSR would be approximately 15% between our ambient (800 μatm) and enriched treatments (1800 μatm) (Figure 12). However, we observed a 103% increase when normalized to LAI at saturating light. Thom (1996) and Beer and Koch (1996) found that at a pH of 8.2, the photosynthetic rate of eelgrass was 21.2 ± 1.7 (SD) and increased to 28.4 ± 3.0 μmol O_2 mg chl^{-1} hr^{-1} (SD) at a pH of 7.8 which corresponds to an approximately 125% increase (Figure 12, Table 3). Similarly, Thom (1996) conducted an experimental trial using similar pH conditions (pH 8.1 and 7.7) and found a 150% increase in photosynthetic rate. However, when Thom (1996) conducted a replicate experimental trial using the same pH conditions, a 20% difference in photosynthetic rate was produced. Therefore, effect of pCO_2 on short-term photosynthetic rates are difficult to measure.

Long-term pCO_2 enrichment effect, on the other hand, is more apparent. For example, Thom (1996) found differences in leaf extension rates between pCO_2 treatments over 7 day trials on whole shoots but could not measure differences in photosynthetic rate during 2-hour trials on leaf clippings. Numerous studies highlight the long-term, positive effects of elevated pCO_2 on the morphology, growth, and proliferation of eelgrass (Thom 1996, Zimmerman et al. 1997, Palacios and Zimmerman 2007, Zimmerman et al. 2017). These findings further support the idea that pCO_2 enrichment effects at these conditions may be present but difficult to detect when the time scale for measurement is short or when the difference in carbonate conditions is moderate.

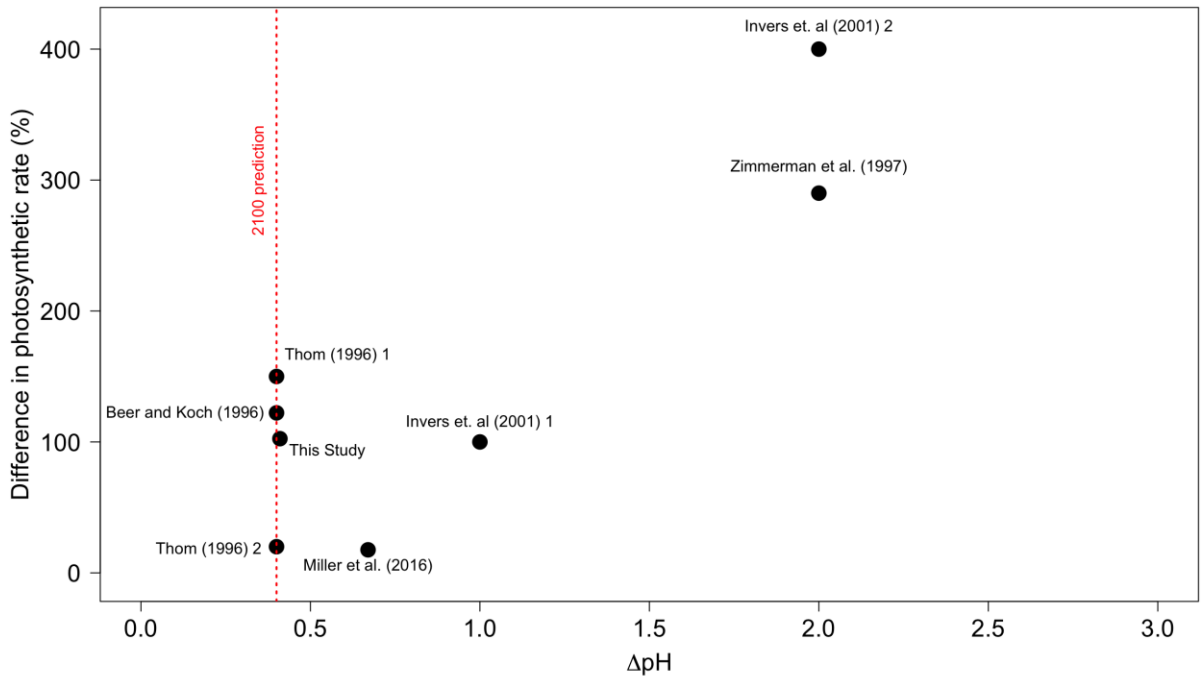

Figure 12. The percent increase in photosynthetic rate (%) with the change in pH associated with those increases of 6 different studies: this study, Beer and Koch (1996), Thom (1996), Zimmerman et al. (1997), Invers et al. (2001), and Miller et al. (2017). We reported Beer and Koch (1996) twice since there were additional treatment levels in their study. Thom (1996) was reported twice since they conducted 2 replicate experiments. Some studies did not report pH values but were calculated using CO_2SYS. The vertical red dashed line represents the change in pH predicted for 2100.

Table 3. Represents the photosynthetic rates reported from different manuscripts. These manuscripts also investigated the effect of enriched pCO_2 on eelgrass but the units for photosynthetic rate and their pCO_2 treatment differences were not similar.

Manuscripts	**Photosynthetic Rate**
Miller et al. (2017)	113 ± 10 (SE) μmol TCO_2 mg chl^{-1} hr^{-1}
Invers et al. (2001)	~3.75 to 7.0 mg O_2 g dw^{-1} hr^{-1}
Beer and Koch (1996)	21.2 ± 1.7 to 28.4 ± 3.0 (SD) μmol O_2 mg chl^{-1} hr^{-1}
Thom (1996)	10 ± 7 to 27 ± 10 (SD) mg O_2 g dw^{-1} hr^{-1}
Zimmerman et al. (1997)	0.3 to 0.78 μmol O_2 mg chl^{-1} min^{-1}

Influence of Light

For pH, Ω_{Ar}, and pCO_2, our models highlight the importance of high LAI and saturating light conditions (H_3) (Table A9). At the highest LAI in our experiment (LAI = 4) and at saturating light, pH, Ω_{Ar}, and pCO_2 increased 0.2 pH units Hr^{-1}, increased 0.45 Ω_{Ar} Hr^{-1}, and decreased 350 μatm Hr^{-1} (Table A9). In Padilla Bay, WA, typical light saturation periods during the summer are approximately 6 hours (Miller et al. 2017). During a typical summer day if these rates held (assuming low water depth and high residence time), eelgrass at high LAI (LAI=4) could increase pH by 1.2 pH units, increase Ω_{Ar} by 2.7 Ω_{Ar}, and decrease pCO_2 by 2,100 μatm (Table A9). The magnitude of this pH change is more than double the expected decreases in surface water pH due to anthropogenic CO_2 (Feely et al., 2004, 2009; Orr et al., 2005; Doney et al., 2009; Steinacher et al., 2009) and changes in pH due to upwelling (Feely et al 2008, Barton et al. 2012). Values as low as 1.2 to 1.5 Ω_{Ar} can compromise biogenic calcification of larval Pacific oysters (Waldbusser et al. 2015), and under favorable conditions, eelgrass photosynthesis can offset this. Furthermore, eelgrass could completely counteract predicted increases in anthropogenic CO_2 (+1000 μatm by 2100) if eelgrass at high LAI (LAI = 4) are given saturating light and a 3-hour residence time and 40 cm water depth.

There is evidence of seasonal patterns of eelgrass morphology and abundance due to changing light conditions where eelgrass productivity is greatest in the summer and lowest in the winter (Dennison and Alberte 1985, Dennison 1987). Therefore, light is often the limiting factor in densely vegetated eelgrass meadows which were generally not thought to be limited by inorganic carbon (Wetzel and Penhale 1983, Dennison and Alberte 1985, Dennison 1987, Borum et al. 2016). Our ambient pCO_2 data (800 μatm) supports the claim that light can limit eelgrass in terms of the rate of carbon uptake at higher LAI values (Figure 7). Similarly, Pajusalu et al. (2016) found that photosynthesis of eelgrass was largely driven by light levels and water temperatures. The saturating light level in this study (PAR = 9.16 ± 0.43 mols m^{-2} d^{-1}) exceeded saturating light requirements established by Thom et al. (2008) (7 mols m^{-2} d^{-1}) for adult eelgrass shoots. Rates of carbon uptake for eelgrass will be the greatest during the summer since the saturating light period is longest compared to winter when day lengths are shorter (Thom 2008). In Padilla Bay during the summer, eelgrass typically experience around 6-hours of saturating light (Miller et al. 2017) which could lead to significant uptake of carbon overall. However, photosynthetically driven changes in carbon uptake and corresponding changes in pH are diel in nature and are usually followed by an opposite and nearly equal decrease in pH due to heterotrophic respiration of organic matter during night time hours (Feely et al. 2008). Net community metabolism processes (photosynthesis and respiration) results in a high frequency oscillation of carbonate chemistry and is overlaid on long-term trends represented by OA (Pacella et al. 2018). This daily variation may bring carbonate chemistry temporarily into favorable conditions each day in the future oceans where baseline conditions have become unfavorable for shellfish and other sensitive organisms, providing a partial amelioration of those conditions for organisms that are capable of capitalizing on these windows of favorable chemistry.

When eelgrass was exposed to sub-saturating light, there were no clear trends observed in the rates of carbon uptake across the range of LAI values tested in this study (Figure 6). The sub-saturating light conditions produced variable rates of carbon uptake of eelgrass like the dark data produced during the initial 3 experimental trials (Figure A1). The variability was likely due to shading or light saturating effects from adjacent tanks that were randomly assigned light treatments (Figure 6). Also, the dark data did not re-produce similar variability as the sub-saturating data since there weren't any light leaks in the overnight experimental trial (Figure 6, Figure A1). Although the light measurements (Table A13) were consistent, the measurements were taken at fixed locations in the center of each tank, which minimize detection of variations in light. The lack of a trend with LAI indicates that there was a methodological problem which explains why significant effects are only found for saturating light conditions.

In the overnight trial in the dark, a small respiration signal was detected which increased with more eelgrass present (Figure 9, Table A10). Although, eelgrass shoots were releasing carbon in the dark, these rates of carbon release were small (about 3.55 ± 0.23 μmol Kg^{-1} Hr^{-1} at a LAI of 4) compared to rates of carbon uptake of eelgrass exposed to saturating light conditions (38.4 ± 1.8 and 57.7 ± 3.1 TCO_2 $Kg^{-1}Hr^{-1}$ for the ambient (800 μatm) and enriched pCO_2 treatments (1800 μatm) respectively at LAI of 4). Our study identified that eelgrass photosynthetic rates increased 10.7x more in saturating light conditions than respiration rates of eelgrass in the dark suggesting that the net primary productivity of eelgrass meadows is positive. Therefore, the contribution of eelgrass meadows to natural respiration processes is relatively small compared to heterotrophic respiration of organic matter. Marsh et al. (1986) also found that photosynthetic rates were 7-12x that of respiration rates of eelgrass at a similar water temperature. Additionally, the eelgrass in this study was incubated hydroponically and sedimentary effects are therefore not considered. Therefore, further

investigation is needed to understand the relative contribution of eelgrass respiration since leaf litter decomposition could be a large source of organic matter for heterotrophic respiration (Harrison and Mann 1975).

Overall, light can dictate photosynthetic rates of eelgrass but light limitations may become more frequent in the future due to anthropogenic sources such as nutrient loading and consequent free floating algae (Eminson and Philips 1978, Sand-Jensen and Borum 1991, Dennison et al. 1993, Short et al. 1995), upland deforestation that can lead to higher turbidity through river transport (Adamus 2014), and sea level rise that can increase the depth of overlying surface waters (Mauger et al. 2015, Miller et al. 2018). Algal blooms initiated by nutrient loading have caused eelgrass to reduce growth, shoot density, average leaf length, and biomass (Short et al. 1995, Moore and Wetzel 2000) and in some cases led to mortality in eelgrass at a given site (Short and Burdick 1996). Therefore, management of water clarity is important to ensure that saturating light conditions reaches eelgrass meadows.

Additional Factors to Consider - Water Temperature

Factors such as water temperature (Zimmerman et al. 1989) could affect rates of carbon uptake in eelgrass meadows and the potential for these meadows to meaningfully change the local conditions. Eelgrass can increase short-term photosynthetic rates at higher water temperatures (Zimmerman et al. 1989). But, photosynthetic rates reach a maximum at a threshold water temperature of approximately 20 ^{o}C (Zimmerman et al. 1989, Pajusalu et al. 2016). Water temperatures above that resulted in greater rates of respiration and 12-fold mortality compared to colder water temperatures (Nejrup and Pederson 2008). Eelgrass meadows will likely experience short-period temperature increases that will exceed their thermal threshold since water temperatures fluctuate diurnally and

can range between 13 to 24 °C at Fidalgo bay and 12 to 21 °C at Cherry Point (Figure A5). Furthermore, the reproductive life cycle of shellfish is also important to consider in tandem with temperature and light variability since shellfish are reproducing during the summer when light and temperatures are also the greatest. Given competing effects of possible future changes in light, pCO_2, and other factors, there is no simple prediction for the increased or decreased potential for eelgrass to drawdown local CO_2 in future oceans.

Additional Factors to Consider - Residence Time and Water Depth

Our results demonstrate the potential of eelgrass to ameliorate OA but these effects were observed at a fixed depth (40-cm) and over a 1-hour residence time which are not necessarily representative of the range of conditions eelgrass meadows experience in the field. Water depth fluctuates naturally based on the tides (3 to 4m range) and at high tide, when water depth is greatest, rates of carbon uptake in eelgrass meadows would have less effect since the amount of carbon removed per liter of seawater is much less (Figure 10) (Mofjeld and Larsen 1984, Lavelle et al. (1988). However, during low tide events, the water depth is smaller and could provide better conditions for photosynthetic activity of eelgrass meadows to exert control over the chemistry of a relatively small amount of water (Figure 10). Currently, the natural range limit of eelgrass in the Salish Sea occurs between 1.3 to -9m (Gaeckle 2009). At any given site the volume of water overlying a patch of eelgrass could vary by more than a factor of 10 over just a few hours during a tidal cycle. Given an eelgrass meadows with an LAI value of 5, rates of carbon uptake for ambient pCO_2 (800 μatm) at a 1m depth are like rates of carbon uptake for enriched pCO_2 (1800 μatm) at a 3m depth (Figure 10). Therefore, if pCO_2 conditions are enriched, eelgrass meadows could take up similar amounts of carbon at deeper depths.

Residence time of water within a meadow is also a key variable in how much influence the meadow can have on water chemistry. Given a longer residence time, photosynthetic activity could have a greater effect on OA conditions (Figure 11). In the Salish Sea, the residence time between basins fluctuate drastically and can range anywhere from approximately 33-44 days in the main basin up to 64 to 121 days in Hood Canal (Babson et al. 2006) or as little as 1-11 days in Bellingham Bay (Wang and Yang 2015). We estimated residence times at Padilla Bay and Willapa Bay based on the meadow sizes from Christaen et al. (2016) and we used current velocity that typically occur in eelgrass meadows (0.5 to 1 m s^{-1}) from Fronseca et al. (1983) assuming currents pass right across based just on meadow size and velocity. In a larger eelgrass meadow, such as Padilla Bay (Bulthuis 1995), the residence time can be approximately 1.5 hours when current velocity is high (1 m s^{-1}). When current velocity is lower (0.5 m s^{-1}), the residence time in Padilla Bay is approximately 3 hours. At Willapa Bay residence times are much smaller due to the smaller coverage of eelgrass (Thom 2003) and the residence time can vary between 0.6 to 1.3 hours based on high and low current velocities (Fonseca et al. 1982, Fonseca et al. 1983).

Residence time in smaller bays or areas of eelgrass, residence times are not as well-studied as larger-scale basins and can vary seasonally due to freshwater inputs (Babson et al. 2006, Sutherland et al. 2011). As a rough estimate for a meadow that is 250 m wide and at a fixed water depth, a tidal current moving water at 0.1 m s^{-1} would result in a residence time of about 40 minutes while a current speed of 0.5 m s^{-1} would result in a residence time of about 8 minutes. Smaller patches, would of course have proportionally shorter residence times. Larger residence times are possible in locations such as Padilla Bay, where the extent of the meadow is extremely large, or possibly under conditions where tidal exchange causes the same parcel of water to leave and reenter a bay several times. If pCO_2 conditions are enriched, the rate of carbon uptake of an eelgrass meadow with an

LAI of 5 and a residence time of 20 minutes would be the same as if the same meadow were exposed to ambient pCO_2 conditions with a 60-minute residence time (Figure 11). Therefore, our results indicate that depth, residence time, LAI, pCO_2, and light are important factors to consider for predicting changes in carbonate chemistry due to eelgrass.

Implications

Our experiment was designed to help inform natural resource managers and policy makers interested in ameliorating the impacts of OA by providing predictive scientific information to help managers make informed decisions about how LAI and pCO_2 influence the ability of eelgrass to take up carbon. This information could inform interpretation of field studies focusing on eelgrass and OA effects. The models we developed in this study can help identify areas of eelgrass that have the most potential to ameliorate OA.

We recommend a cautious approach to the use of eelgrass as a strategy for ameliorating OA conditions since the conditions under which this is feasible are specific, and sometimes short lived. If managers do wish to pursue the idea, identifying shellfish restoration sites that are adjacent to eelgrass meadows with high LAI values (LAI = 4), large area, moderate water depths, and high residence times are important factors to consider. Water clarity must also be accounted for since saturating light is a key driver in determining the rate of carbon uptake of eelgrass. Enriched pCO_2 conditions could potentially be ameliorated by eelgrass, given that the meadows have high LAI. But, short-residence times and larger depths could diminish the pCO_2 effect on photosynthetic rates.

Overall, these results help us understand the observed pH variability in the field and the mechanisms that drive pH variability in the nearshore. The rates of change identified based on our experimental models can be combined with other models predicting the variability of pH throughout the Salish Sea.

Key Points

1. The ability of eelgrass meadows to influence localized carbonate chemistry through carbon uptake is driven largely by LAI and light and mediated by water depth and residence time.
2. Evidence for an increase in photosynthetic rate in response to increased TCO_2 is mixed. It is likely that an effect exists but the magnitude is small and difficult to detect when changes in TCO_2 are modest, or when LAI is small.
3. Other changes in the Salish Sea related to climate change and human influence may have the potential to decrease the ability of eelgrass meadows to ameliorate localized carbonate chemistry conditions.
4. Eelgrass meadows where residence time is generally longer, the ratio of eelgrass to water is large, and the eelgrass LAI is high. Meadows that fit these criteria have the greatest potential for drawing down carbon in local waters but are not common. But, sites such as Padilla Bay, Nisqually Reach, and Willapa Bay are most likely to fit these criteria.

References Cited

Adamus P (2014) Effects of Forest Roads and Tree Removal In or Near Wetlands of the Pacific Northwest: A Literature Synthesis. Cooperative Monitoring Evaluation and Research Report CMER 12-1202. Washington State Forest Practices Adaptive Management Program. Washington Department of Natural Resources, Olympia, WA.

Altman N and Krzywinski M (2016) Points of significance: Analyzing outliers: Influential or nuisance? 281.

Babson AL, Kawase M, & MacCready P (2006) Seasonal and Interannual Variability in the Circulation of Puget Sound, Washington: A Box Model Study. *Atmosphere-Ocean*, 44(1), 29–45.

Backman TW, and Barilotti DC (1976) Light reduction: effects on standing crops of the eelgrass *Zostera marina* in a coastal lagoon. *Marine Biology* 34:33-40.

Barko JW, Hardin DG, Matthews MS (1982) Growth and morphology of submersed freshwater macrophytes In relation to light and temperature. *Can. J. Bot.* 60: 877-887

Barton A, Hales B, Waldbusser GG, Langdon C, and Feely RA (2012) The Pacific oyster, *Crassostrea gigas*, shows negative correlation to naturally elevated carbon dioxide levels: Implications for near-term ocean acidification effects. *Limnology and Oceanography* 57:698–710.

Barton A, Waldbusser G, Feely R, Weisberg S, Newton J, McLauglin K (2015) Impacts of Coastal Acidification on the Pacific Northwest Shellfish Industry and Adaptation Strategies Implemented in Response. *Oceanography*, 25(2), 146–159.

Beer S and Koch E (1996) Photosynthesis of marine macroalgae and seagrasses in globally changing CO_2 environments. *Marine Ecology Progress Series* 141:199–204

Beer S and Rehnberg J (1997) The acquisition of inorganic carbon by the seagrass *Zostera marina*. *Aquatic Botany* 56:277–283.

Black KP, Gay SL, and Andrews JC (1990) Residence times of neutrally-buoyant matter such as larvae, sewage or nutrients on coral reefs *Coral Reefs* 9 109–14

Borges AV and Frankignoulle M (1999) Daily and seasonal variations of the partial pressure of CO_2 in surface seawater along Belgian and southern Dutch coastal areas. *Journal of Marine Systems* 19:251–266.

Borum J, Pedersen O, Kotula L, Fraser MW, Statton J, Colmer TD, & Kendrick GA (2016) Photosynthetic response to globally increasing CO2 of co-occurring temperate seagrass species. *Plant, Cell & Environment* 39(6), 1240–1250.

Bulthuis DA (1990) Leaf surface area. In Seagrass Research Methods, pp.69–79. Phillips RC and McRoy CP(editors). Paris, France: United Nations Educational, Scientific and Cultural Organization.

Bulthuis DA (1995) Distribution of seagrasses in a North Puget Sound estuary: Padilla Bay, Washington, USA. *Aquatic Botany* 50(1), 99–105.

Busch DS, Chris J. Harvey, Paul McElhany (2013) Potential impacts of ocean acidification on the Puget Sound food web. *ICES Journal of Marine Science*, Volume 70, Issue 4, Pages 823–833.

Busch DS, McElhany P (2016) Estimates of the Direct Effect of Seawater pH on the Survival Rate of Species Groups in the California Current Ecosystem. *PLoS ONE* 11(8)

Cai W-J and Wang Y (1998) The chemistry, fluxes, and sources of carbon dioxide in the estuarine waters of the Satilla and Altamaha Rivers, Georgia. *Limnology and Oceanography* 43(4), 657–668.

Cai WJ, Pomeroy LR, Moran MA, and Wang Y (1999) Oxygen and carbon dioxide mass balance for estuarine-intertidal marsh complex of five rivers in the southeastern U.S. *Limnol. Oceanogr.* 44, 639–649.

Caldeira K and Wickett ME, (2003) Oceanography: Anthropogenic carbon and ocean pH. *Nature* 425, 365

Caldeira K and Wickett ME (2005) Ocean model predictions of chemistry changes from carbon dioxide emissions to the atmosphere and ocean. *Journal of Geophysical Research.* Oceans. 10:C9.

Canadell JG, Le Quere C, Raupach MR, Field CB, Buitenhuis ET, Ciais P, Conway TJ, Gillett NP, Houghton RA, Marland G (2007) Contributions to accelerating atmospheric CO_2 growth from economic activity, carbon intensity, and efficiency of natural sinks. Proceedings of the National Academy of Sciences of the United States of America 104, 18866e18870

Carr LA, Boyer KE, and Brooks AJ (2011) Spatial patterns of epifaunal abundance in San Francisco Bay eelgrass (*Zostera marina*) beds. *Marine Ecology*. 32:88–103.

Christiaen B, Dowty P, Ferrier L, Gaeckle J, Berry H, Stowe J, Sutton E (2016) Puget Sound Submerged Vegetation Monitoring Program - 2014 Report

Clayton TD and Byrne RH (1993) Spectrophotometric seawater pH measurements-total hydrogen-ion concentration scale calibration of M-cresol purple and at sea results. *Deep-Sea Research* 40:2115–2129.

Dennison WC and Alberte RS (1985) Role of daily light period in the depth distribution of *Zostera marina* (eelgrass). *Mar. Ecol. Prog. Ser.* 25: 51-61.

Dennison WC (1987) Effects of light on seagrass photosynthesis, growth and depth distribution. *Aquatic Botany* 27.1: 15-26.

Dennison WC (1990) Chlorophyll content. In: R.C. Phillips and C.P. McRoy (eds) *Seagrass Research Methods*. Unesco, Paris, France, pp.83-85.

Dennison WC, et al. (1993) Assessing water quality with submersed aquatic vegetation. *BioScience* 43.2: 8694.

Dickson A and Millero F (1987) A Comparison of the Equilibrium Constants for the Dissociation of Carbonic Acid in Seawater Media. *Deep-Sea Research* 34:1733–1743.

Dickson AG, Sabine CL and Christian JR (Eds.) (2007) Guide to Best Practices for Ocean CO_2 Measurements. *PICES Special Publication* 3 191 pp.

Doney SC, Fabry VJ, Feely RA, and Kleypas JA (2009) Ocean Acidification: The Other CO_2 Problem. *Annual Review of Marine Science* 1:169–192.

Duarte CM and Kalff J (1987) Weight-density relationships in submerged macrophytes. The importance of light and plant geometry. *Oecologia* 72: 612-617

Duarte CM (1991) Seagrass depth limits. *Aquatic Botany* 40: 363-377.

Duarte CM, Marbà N, Gacia E, Fourqurean JW, Beggins J, Barrón C, and Apostolaki ET (2010) Seagrass community metabolism: Assessing the carbon sink capacity of seagrass meadows. *Global Biogeochemical Cycles*. 24:GB4032.

Dumbauld, BR, Kauffman BE, Trimble A, & Ruesink JL (2011) The Willapa Bay oyster reserves in Washington state: Fishery collapse, creating a sustainable replacement, and the potential for habitat conservation and restoration. *J. Shellfish Res* 30: 71–83

Echavarria-Heras H, Lee KS, Solana-Arellano E, and Franco-Vizcaíno E (2011) Formal analysis and evaluation of allometric methods for estimating above-ground biomass of eelgrass. *Annals of Applied Biology* 159:503–515.

Eminson D and Philips G (1978) A laboratory experiment to examine the effects of nutrient enrichment on macrophyte and epiphyte growth. *Int. Verh. Limnol.*, 20:82-87.

Fabry VJ, Seibel BA, Feely RA, Orr JC (2008) Impacts of ocean acidification on marine fauna and ecosystem processes. *ICES Journal of Marine Science* 65:414–432.

Feely RA, Sabine CL, Lee K, Berelson W, Kleypas J, Fabry VJ, and Millero FJ (2004) Impact of anthropogenic CO_2 on the $CaCO_3$ system in the oceans. Science 305:362–366.

Feely RA, Sabine CL, Hernandez-Ayon M, Lanson D and Hales B (2008) Evidence for upwelling of corrosive acidified water onto the continental shelf. *Science* 320:1490-1492.

Feely RA, Doney SC, and Cooley SR, (2009) Ocean acidification: Present conditions and future changes in a high-CO_2 world. *Oceanography* 22, 36-47.

Feely RA, Alin SR, Newton J, Sabine CL, Warner M, Devol A, Krembs C, and Maloy C (2010) The combined effects of ocean acidification, mixing, and respiration on pH and carbonate saturation in an urbanized estuary. Estuarine *Coastal and Shelf Science* 88:442–449.

Fonseca MS., Fisher JS, Zieman JC, and Thayer GW (1982) Influence of the seagrass*, Zostera marina* L., on current flow. *Estuarine, Coastal and Shelf Science* 15(4), 351–364.

Fonseca MS, Zieman JC, Thayer GW, and Fisher JS (1983) The role of current velocity in structuring eelgrass (*Zostera marina* L.) meadows. *Estuarine, Coastal and Shelf Science* 17(4), 367–380.

Frankignoulle M, Abril G, Borges A, Bourge I, Canon C, Delille B, Libert E, and Théate JM (1998) Carbon dioxide emission from European estuaries. *Science* 282, 434–436.

Gaeckle J, Dowty P, Berry H and Ferrier L (2009) Puget Sound Submerged Vegetation Monitoring Project 2008 Monitoring Report. Nearshore Habitat Program, Washington State Department of Natural Resources. Olympia, WA. 57pp.

Guinotte JM and Fabry VJ (2008) Ocean acidification and its potential effects on marine ecosystems. *Annals of the New York Academy of Sciences* 1134:320-342.

Hale R, et al. (2011) Predicted levels of future ocean acidification and temperature rise could alter community structure and biodiversity in marine benthic communities. *Oikos* 120.5: 661-674.

Harris KE, DeGrandpre MD, and Hales B (2013) Aragonite saturation state dynamics in a coastal upwelling zone. *Geophysical Research Letters* 40.11: 2720-2725.

Harrison PG, and Mann KH (1975) Detritus formation from eelgrass (*Zostera marina* L.): the relative effects of fragmentation, leaching, and decay. *Limnology and Oceanography* 20.6: 924-934.

Hedges JI, Keil RG, and Benner R (1997) What happens to terrestrial organic matter in the ocean? *Organic geochemistry* 27:195-212.

Hendriks IE, Olsen YS, Ramajo L, Basso L, Steckbauer A, Moore TS, Howard J, Duarte CM (2014) Photosynthetic activity buffers ocean acidification in seagrass meadows. *Biogeosciences* 11:333–346.

Hill VJ, Zimmerman RC, Bissett WP, Dierssen H, & Kohler DD (2014) Evaluating light availability, seagrass biomass, and productivity using hyperspectral airborne remote sensing in Saint Joseph's Bay, Florida. *Estuaries and Coasts* 1–23.

Hinga KR (2002) Effects of pH on coastal marine phytoplankton. *Marine Ecology Progress Series* vol. 238 pg. 281-300

Iglesias-Rodrıguez MD, Halloran PR, Rickaby REM, Hall IR, Colmenero-Hidalgo E, et al. (2008) Phytoplankton calcification in a high CO_2 world Science 320:336–39

Inskeep WP & Bloom PR (1985) Extinction Coefficients of Chlorophyll a and b in N, N-Dimethylformamide and 80% Acetone. *Plant Physiology* 77(2), 483–485.

Invers O, et al. (2001) Inorganic carbon sources for seagrass photosynthesis: an experimental evaluation of bicarbonate use in species inhabiting temperate waters. *Journal of Experimental Marine Biology and Ecology* 265.2: 203-217.

IPCC. 2014. Climate Change (2014) Synthesis Report. Contribution of Working Groups I, II and III to the Fifth Assessment Report of the Intergovernmental Panel on Climate Change [Core Writing Team, Pachauri RK and Meyer LA (eds.)]. IPCC, Geneva, Switzerland, 151 pp.

Jokiel PL, Bahr KD, Rodgers KS (2014) Low-cost, high-flow mesocosm system for simulating ocean acidification with CO_2 gas. *Limnology and Oceanography Methods* 12:313-322.

Kroeker KJ, Kordas RL, Crim RN, and Singh GG (2010) Meta-analysis reveals negative yet variable effects of ocean acidification on marine organisms. *Ecology Letters* 13: 1419–1434.

Lavelle JW, Mofjeld HO, Lempriere-Doggett E, Cannon GA, Pashinski DJ, Cokelet ED, Lytle L, and Gill S (1988) A multiply-connected channel model of tides and tidal currents in Puget Sound, Washington and a comparison with updated observations. NOAA Tech. Memo. ERL PMEL-84, Pacific Marine Environmental Laboratory, NOAA.

van Lent F and Verschuure JM (1994) Intraspecific variability in *Zostera marina* L. (eelgrass) in the estuaries and lagoons of the southwestern Netherlands. I. Population dynamics. *Aquat. Bot.* 48: 31–58.

Manzello DP, Enochs IC, Melo N, Gledhill DK, and Johns EM (2012) Ocean Acidification Refugia of the Florida Reef Tract. *PLOS ONE* 7:e41715.

Marsh J, William A, Dennison C, and Alberte RS (1986) Effects of temperature on photosynthesis and respiration in eelgrass (*Zostera marina* L.). *Journal of Experimental Marine Biology and Ecology* 101:257-267.

Mauger GS, Casola JH, Morgan HA, Strauch RL, Jones B, Curry B, Busch TM, Isaksen L, Binder W, Krosby MB, and Snover AK (2015) State of Knowledge: Climate Change in Puget Sound. Report prepared for the Puget Sound Partnership and the National Oceanic and Atmospheric Administration. Climate Impacts Group, University of Washington, Seattle.

Mazzella L, and Alberte RS (1986) Light adaptation and the role of autotrophic epiphytes in primary production of the temperate seagrass, *Zostera marina* L. *Journal of Experimental Marine Biology and Ecology* 100.1-3: 165-180.

Mehrbach C, Culberso CH, Hawley J, and Pytkowic RM (1973) Measurement of Apparent Dissociation Constants of Carbonic Acid in Seawater at Atmospheric Pressure. *Limnology and Oceanography* 18:897–907.

Meehl GA, Stocker TF, Collins WD, Friedlingstein P, Gaye AT, Gregory JM, Kitoh A, Knutti R, Murphy JM, Noda A, Raper SCB, Watterson IG, Weaver AJ and Zhao ZC (2007) Global Climate Projections. I: Climate Change 2007: The Physical Science Basis. Contribution of Working Group I to the Fourth Assessment Report of the Intergovernmental Panel on Climate Change. Solomon S, Qin D, Manning M, Chen Z, Marquis M, Averyt KB, Tignor M and Miller HL (editors). Cambridge University Press, Cambridge, United Kingdom and New York, NY, USA.

Miller CA, Yang S, & Love BA (2017) Moderate Increase in TCO_2 Enhances Photosynthesis of Seagrass *Zostera japonica*, but Not *Zostera marina*: Implications for Acidification Mitigation. *Frontiers in Marine Science* 4.

Miller IM, Morgan H, Mauger G, Newton T, Weldon R, Schmidt D, Welch M, Grossman E (2018) Projected Sea Level Rise for Washington State – A 2018 Assessment. A collaboration of Washington Sea Grant, University of Washington Climate Impacts Group, Oregon State University, University of Washington, and US Geological Survey. Prepared for the Washington Coastal Resilience Project.

Mofjeld HO and Larsen LH (1984) Tides and Tidal Currents of the Inland Waters of Western Washington. NOAA Tech. Memo. ERL PMEL-56, Pacific Marine Environmental Laboratory, NOAA.

Moore KA and Wetzel RL (2000) Seasonal variations in eelgrass *(Zostera marina L.)* responses to nutrient enrichment and reduced light availability in experimental ecosystems. *Journal of Experimental Marine Biology and Ecology 244(1), 1–28*.

Mucci A (1983) The solubility of calcite and aragonite in seawater at various salinities, temperatures, and one atmosphere total pressure. *American Journal of Science* 283.

Nejrup LB, and Pedersen MF (2008) Effects of salinity and water temperature on the ecological performance of *Zostera marina*. *Aquatic Botany* 88.3: 239-246.

NOAA/ESRL, Ed Dlugokencky and Pieter Tans (2016) (www.esrl.noaa.gov/gmd/ccgg/trends/)

Olesen B and Sand-Jensen K (1993) Seasonal acclimatization of eelgrass *Zostera marina* growth to light. *Marine Ecology-Progress Series* 94 (1993): 91-91.

Olesen B and Sand-Jensen K (1994) Demography of shallow eelgrass (*Zostera marina*) populations—shoot dynamics and biomass development. *Journal of Ecology*: 379-390.

Orr JC, Fabry VJ, Aumont O, Bopp L, Doney SC, Feely RA, Gnanadesikan A, Gruber N, Ishida A, Joos F, Key RM, Lindsay K, Maier-Reimer E, Matear R, Monfray P, Mouchet A, Najjar RG, Plattner GK, Rodgers KB, Sabine CL, Sarmiento JL, Schlitzer R, Slater RD, Totterdell IJ, Weirig MF, Yamanaka Y, and Yool A (2005) Anthropogenic ocean acidification over the twenty-first century and its impact on calcifying organisms. *Nature* 437:681–686.

Pacella SR, Brown CA, Waldbusser GG, Labiosa RG, and Hales B (2018) Seagrass habitat metabolism increases short-term extremes and long-term offset of CO_2 under future ocean acidification. *Proceedings of the National Academy of Sciences* 115(15)

Palacios SL and Zimmerman RC (2007) Response of eelgrass *Zostera marina* to CO_2 enrichment: possible impacts of climate change and potential for remediation of coastal habitats. *Marine Ecology Progress Series* 344: 1-13.

Palmer AR (1992) Calcification in marine mollusks—how costly is it? Proc. *Natl. Acad. Sci.* 89: 1379–1382.

Pajusalu L, Martin G, Põllumäe A, and Paalme T (2016) The Influence of CO_2 Enrichment on Net Photosynthesis of Seagrass *Zostera marina* in a Brackish Water Environment. *Frontiers in Marine Science* 3.

Phillips RC, McMillan C, and Bridges KW (1983) Phenology of eelgrass, *Zostera marina* L. along latitudinal gradients in North America. Aquatic Botany 15:145-156.

Pierrot D, Lewis E, and Wallace DWR (2006) MS Excel Program Developed for CO_2 System Calculations. ORNL/CDIAC-105a. Carbon Dioxide Information Analysis Center, Oak Ridge National Laboratory, U.S. Department of Energy, Oak Ridge, Tennessee.

R Core Team (2016). R: A language and environment for statistical computing. R Foundation for Statistical Computing, Vienna, Austria. URL https://www.R-project.org/.

Ries JB, Cohen AL, and McCorkle DC (2008) Marine biocalcifiers exhibit mixed responses to CO_2 induced ocean acidification. 11th Int. Coral Reef Symp., Ft. Lauderdale.

Royal Society. 2005. Ocean acidification due to increasing atmospheric carbon dioxide. London: the Royal Society. 57 p.

Sand-Jensen K & Borum J (1991) Interactions among phytoplankton, periphyton and macrophytes in temperate freshwater and estuaries, *Aquatic Botany*, 41, pp. 137-175.

Short FT, Burdick DM, Wolf J, Jones GE, (1993) Eelgrass in Estuarine Research Reserves Along the East Coast, USA, Part I: Declines from Pollution and Disease and Part II: Management of Eelgrass Meadows. NOAA, Coastal Ocean Program Publ., p. 107.

Short FT, Burdick DM, and Kaldy JE. (1995) Mesocosm experiments quantify the effects of eutrophication on eelgrass, *Zostera marina*. *Limnology and oceanography* 40.4: 740-749

Short FT, Burdick DM, Granger S, and Nixon SW (1996) Long-term decline in eelgrass, *Zostera marina* L., linked to increased housing development, p. 291-298. In J. Kus, R. C. Phillips, D. I. Walker, and H. Kirkman (eds.), Seagrass Biology: Proceedings of an International Workshop. Sciences UWA, Nedlands, Western Australia.

Short FT & Wyllie-Echeverria S (1996) Natural and human-induced disturbance of seagrasses. *Environmental Conservation* 23(01), 17.

Short FT & Duarte CM (2001) Methods for the measurement of seagrass growth and production. *Global Seagrass Research Methods*, 155–182.

Solana-Arellano E, Echavarria-Heras H, and Gallegos-Martinez ME (2003) Improved leaf area index based biomass estimations for *Zostera marina* L. IMA *Journal of Mathematical Medicine and Biology* 20:367–375.

Solomon S, et al. (2007) Climate change 2007-the physical science basis: Working group I contribution to the fourth assessment report of the IPCC. Vol. 4. Cambridge university press.

Steinacher M, Joos F, Frölicher TL, Plattner G-K, & Doney SC (2009) Imminent ocean acidification in the Arctic projected with the NCAR global coupled carbon cycle-climate model. *Biogeosciences* 6(4), 515–533.

Stevens TS, Apple JA, Alexander GA, Angell CA, and Riggs SR (2016) Padilla Bay National Estuarine Research Reserve Management Plan. Washington State Department of Ecology, Shorelands and Environmental Assistance Program, Padilla Bay NERR, Mount Vernon, Washington.

Sutherland DA, MacCready P, Banas NS, and Smedstad LF (2011) A Model Study of the Salish Sea Estuarine Circulation. *Journal of Physical Oceanography* 41(6), 1125–1143.

Thom, R. M. (1996). CO_2-Enrichment effects on eelgrass (*Zostera marina* L.) and bull kelp (*Nereocystis luetkeana* (mert.) P & R.). *Water, Air, and Soil Pollution* 88(3-4), 383–391.

Thom RM, et al. (2003) Factors influencing spatial and annual variability in eelgrass (*Zostera marina* L.) meadows in Willapa Bay, Washington, and Coos Bay, Oregon, estuaries. *Estuaries* 26.4: 1117-1129.

Thom RM, Southard SL, Borde AB, and Stoltz P (2008) Light Requirements for Growth and Survival of Eelgrass (Zostera marina L.) in Pacific Northwest (USA) Estuaries. *Estuaries and Coasts* 31(5), 969–980.

Trenberth K (1996) The climate system: an overview. In: Houghton JT, Meira Filho LG, Callader BA, Harris N, Kattenberg A, Maskell K (eds) Climate change 1995: the science of climate change. Cambridge University Press, New York

Unsworth RKF, Collier CJ, Henderson GM, and McKenzie LJ (2012) Tropical seagrass 55 meadows modify seawater carbon chemistry: implications for coral reefs impacted by ocean acidification. *Environmental Research Letters* 7:024026.

Waldbusser GG, et al. (2015) Saturation-state sensitivity of marine bivalve larvae to ocean acidification. *Nature Climate Change* 5.3: 273.

Wang T and Yang Z (2015) Understanding the flushing capability of Bellingham Bay and its implication on bottom water hypoxia. *Estuarine Coastal and Shelf Science* 165, 279–290.

Wetzel RL and Penhale PA (1983) Production ecology of seagrass communities in the lower Chesapeake Bay. *Mar. Tech. Soc. J* 17(2): 22--31.

Wicaksono P and Hafizt M (2013) Mapping seagrass from space: Addressing the complexity of seagrass LAI mapping. *European Journal of Remote Sensing* 46.1: 18-39.

Wootton JT, Pfister CA, and Forester JD (2008) Dynamic patterns and ecological impacts of declining ocean pH in a high-resolution multi-year dataset. *Proceedings of the National Academy of Sciences* 105:18848–18853

Yang S, Wheat EE, Horwith MJ, and Ruesink JL (2013) Relative impacts of natural stressors on life history traits underlying resilience of intertidal eelgrass (*Zostera marina* L.). *Estuaries and coasts* 36:1006-1013.

Zimmerman RC, Smith RD, and Alberte RS (1989) Thermal acclimation and whole-plant carbon balance in *Zostera marina* L. (eelgrass). *Journal of Experimental Marine Biology and Ecology* 130(2), 93–109.

Zimmerman RC, Reguzzoni JL, Wyllie-Echeverria S, Josselyn M and Alberte RS (1991) Assessment of environment suitability for growth of *Zostera marina* L. (eelgrass) in San Franscisco Bay. *Aquat. Bot.* 39: 353–366.

Zimmerman RC, Reguzzoni JL, and Alberte RS (1995) eelgrass (*Zostera marina* L.) transplants in San Francisco Bay: role of light availability on metabolism, growth and survival. *Aquatic Botany* 51:67-86.

Zimmerman RC, Kohrs DG, Steller DL, and Alberte RS. (1997) Impacts of CO_2 enrichment on productivity and light requirements of eelgrass. *Plant Physiology* 115:597-607.

Zimmerman RC, et al. (2017) Experimental impacts of climate warming and ocean carbonation on eelgrass *Zostera marina*. *Marine Ecology Progress Series* 566 (2017): 1-15.

Appendix

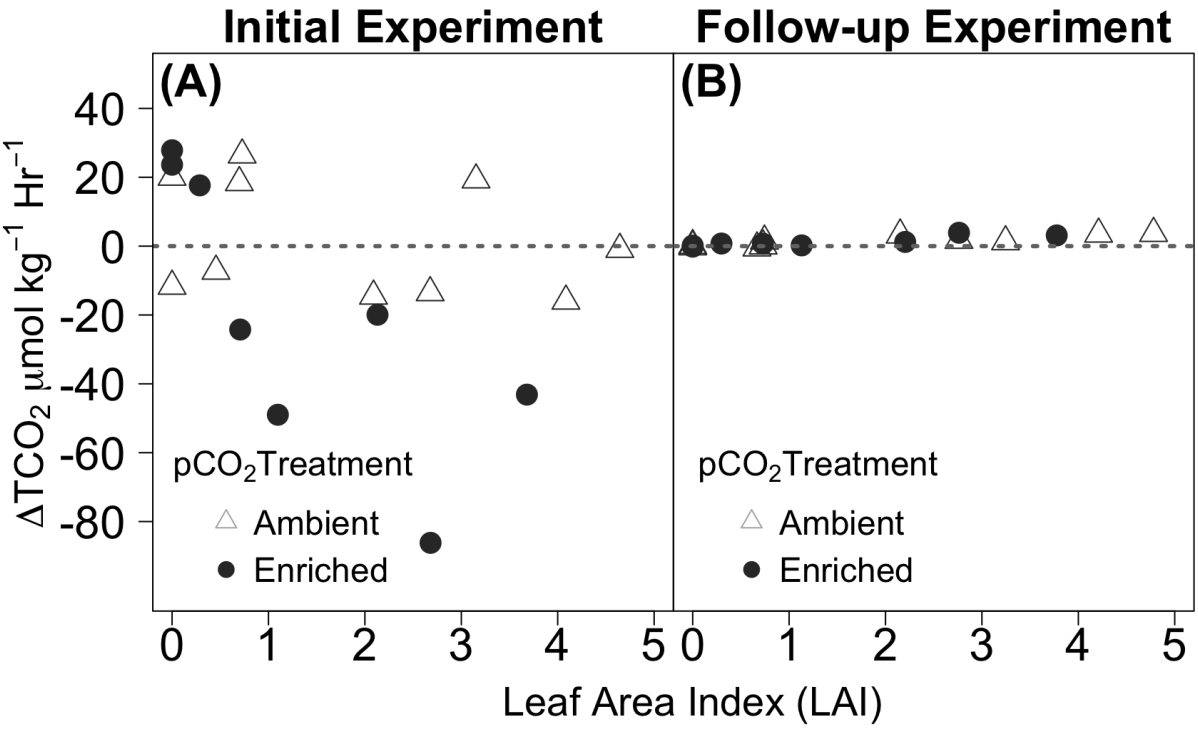

Figure A1. The dark condition produced extremely variable changes in TCO_2 (umol kg^{-1} Hr^{-1}) in the mixed light treatment (saturating and sub-saturating) experimental runs (A) compared to the night-time experimental trial where all tanks were incubated in the dark overnight for 9-hours (B). We discarded the dark data from the mixed light treatment experiment and ran a separate analysis from the saturating and sub-saturating data for the follow-up dark experiment. The variation in the initial experiment was thought to be due to light leaks into dark tanks from nearby saturating and sub-saturating light treatment tanks.

Table A1. Summary output of the Shapiro-Wilk Normality test for leaf area index as a function of Site and elevation (test) with the following test statistic (*W*), and *p*-value.

Test	Test statistic (*W*)	*p*-value
LAI ~ Site	0.98	0.695
LAI ~ Elevation	0.91	0.086

Table A2. Summary output of Leven's test for homogenous variance for leaf area index as a function of site and elevation with the following degrees of freedom (*df*), F value, and *p*-value.

Test	*df*	F value	*p*-value
LAI ~ Site	6, 67	0.98	0.094
LAI ~ Elevation	5, 12	1.11	0.403

Table A3. Chi-square test summary output for the leaf area index across different elevations at Padilla Bay and the output for the leaf area index across different sites in Washington State. The factor, degrees of freed (*df*), sums of squares (Sum Sq), F value, and *p*-values are shown.

Factor	*df*	Sum Sq	Mean Sq	F value	*p*-value
Elevation	5	43.65	8.73	16.41	<0.001
Residuals	12	6.39	0.53		
Site	5	63.84	12.77	12.37	<0.001
Residuals	50	51.59	1.032		

Table A4. Outputs of the orthogonal contrasts tested on field observations of leaf area index (LAI). We compared the LAI between different sites throughout Washington State and between different elevations within Padilla Bay, WA. The contrast of different factor levels, degrees of freedom (*df*), sums of squares (Sum Sq), mean squares (Mean Sq), F value, and *p*-value are shown.

Contrast	*df*	Sum Sq	Mean Sq	F value	p-value
Site (main effect)	5	63.84	12.77	12.37	<0.001
high vs low	1	16.21	16.21	15.71	<0.001
Residuals	50	51.59	1.032		
Elevation (main effect)	5	43.65	8.73	16.41	<0.001
+1 to 0 vs. 0 to -1	1	8.01	8.01	15.06	0.002
0 to -1 vs. -1 to -2	1	3.85	3.85	7.24	0.019
+1 to 0 vs. -1 to -2	1	5.18	5.18	9.737	0.009
Residuals	12	6.39	0.53		

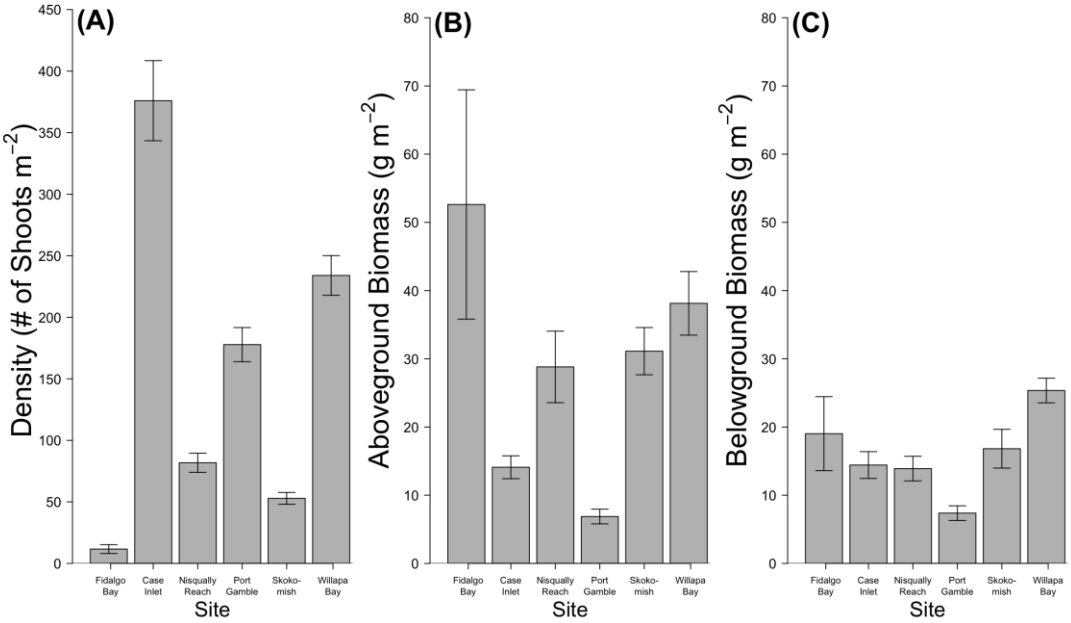

Figure A2. Field observations of (A) shoot density (# of shoots m^{-2}), (B) aboveground biomass (g m^{-2}), and (C) belowground biomass (g m^{-2}) of sites: Fidalgo Bay, Case Inlet, Nisqually Reach, Port Gamble, Skokomish, and Willapa Bay where all sites had a sample size of 9 except for Fidalgo Bay which had a sample size of 12.

Table A5. Model summary of uncorrected data (raw ΔTCO_2~LAI*CO_2*Light) including the factor, estimate, standard error (SE), t-value, *p*-value using the maximum likelihood estimation and excluding the dark data.

Factor	Estimate	SE	t-value	*p*-value
(Intercept)	**-14.682**	**3.239**	**-4.53**	**<0.001**
LAI	-0.564	1.271	-0.44	0.661
CO_2 (Enriched)	-1.551	4.702	-0.33	0.744
Light (Saturating)	6.534	4.58	1.43	0.165
LAI:CO_2 (Enriched)	1.67	2.205	0.76	0.455
LAI:Light (Saturating)	**-7.128**	**1.798**	**-3.96**	**<0.001**
CO_2 (Enriched):Light (Saturating)	10.035	6.649	1.51	0.142
LAI: CO_2 (Enriched):Light (Saturating)	**-7.304**	**3.118**	**-2.34**	**0.027**

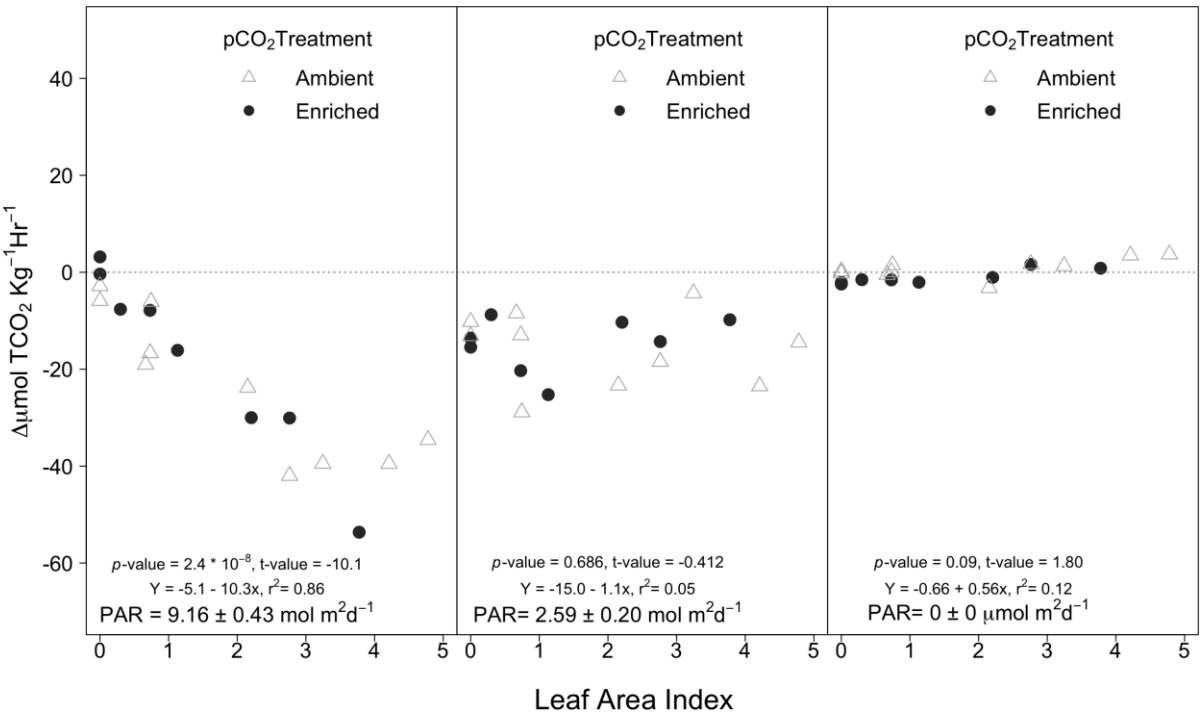

Figure A3. Raw data for the change in the total carbon uptake (raw ΔTCO_2 μmol kg^{-1} Hr^{-1}) compared to the LAI of eelgrass ranging from 0 to 5 for saturating, sub-saturating and dark irradiance levels (left, middle, and right panels). Open triangles represent ambient pCO_2 (800 μatm) and closed circles represent enriched pCO_2 (1800 μatm). The solid red line represents the linear regression and the dashed red line represents 95% CI. The mean differences in control tanks (LAI= 0) were adjusted to zero and this correction was applied to all tanks where the difference was +4.368, -11.679, and 0.008 μmol kg^{-1} Hr^{-1} for the ambient pCO_2 response and -1.395, -14.520, and -20.505 μmol kg^{-1} Hr^{-1} for the enriched pCO_2 response for saturating, sub-saturating and dark irradiance levels respectively. Outputs from each linear model is reported in the bottom left corner of each panel.

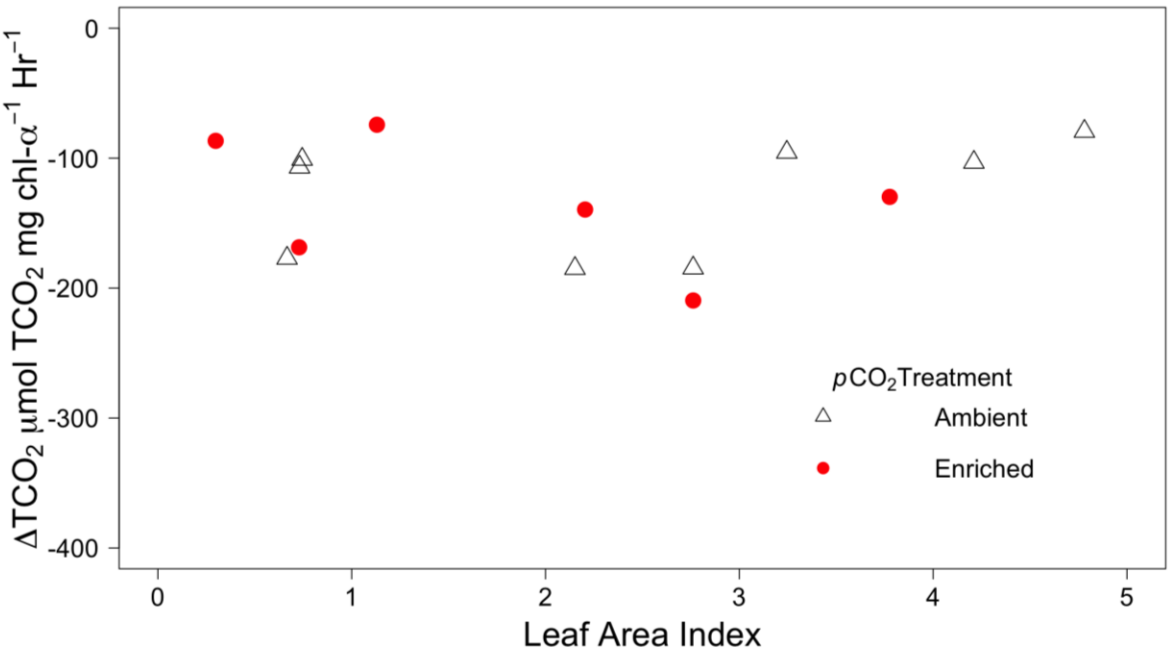

Figure A4. The change in carbon uptake normalized to the amount of chlorophyll estimated per tank (ΔTCO_2 µmol TCO_2 mg chl-a^{-1} Hr^{-1} across leaf area index (LAI) values. The ambient pCO_2 treatment (800 µatm) is represented by black triangles and the enriched pCO_2 treatment (1800 µatm) is represented by solid red circles.

Table A6. Summary output for ΔTCO_2 (µmol TCO_2 Kg^{-1} Hr^{-1}) normalized to the amount of chlorophyll per tank (mg chl^{-1}). Factor, Value, standard error (SE), t-value, and *p*-value are represented below.

Factor	**Value**	**SE**	**t-value**	***p*-value**
(Intercept)	-76.40	65.92	-1.16	0.260
LAI	9.86	23.14	0.43	0.675
CO_2 (Enriched)	-59.23	58.28	-1.66	0.061
Light (Saturating)	-77.15	93.22	-0.82	0.418
LAI:CO_2 (Enriched)	115.02	40.61	2.83	0.102
LAI:Light (Saturating)	-150.31	32.73	0.01	0.032
CO_2 (Enriched):Light (Saturating)	0.314	138.99	2.93	0.845
LAI:CO_2 (Enriched):Light (Saturating)	-141.08	57.42	-2.46	0.231

Table A7. Model selection – comparing linear versus quadratic models for predicting changes in the rate of total carbon uptake (ΔTCO_2 μmol kg^{-1} Hr^{-1}) as a function of leaf area index (LAI). The model equation, degrees of freedom (*df*), akaike information criterion (AIC), bayesian information criterion (BIC), log likelihood (logLik), test, liklihood-ratio test (L.Ratio), and the *p*-value are reported.

pCO_2 Treatment	Model	*df*	AIC	BIC	logLik	Test	L.Ratio	*p*-value
Ambient (800 μatm)	Linear	3	66.4	66.7	-30.2	Linear vs. Quadratic		
	Quadratic	4	61.7	61.4	-26.8		6.79	0.009
Enriched (1800 μatm)	Linear	3	43.6	42.9	-18.8	Linear vs. Quadratic		
	Quadratic	4	43.3	41.7	-17.6		2.31	0.129

Table A8. Summary output for the quadratic model fit for the ambient pCO_2 treatment (800 μatm). Here we report the factor, value, standard error (SE), t-value, and *p*-values. The quadratic formula is $Y = 2.25x^2 - 17.84x - 3.16$.

ΔTCO_2 ~ LAI + LAI^2 (Ambient pCO_2)

Factor	Value	SE	t-value	*p*-value
(Intercept)	-3.16	3.39	-0.932	0.3823
LAI	-17.84	4.11	-4.337	0.0034
LAI^2	2.25	0.88	2.56	0.0376

Table A9. Model selection summary using the likelihood-ratio test to assess the random variance structure (experimental trial and tank) of our model using the residual maximum likelihood estimation method (REML) and to assess covariate effects (change in water temperature) in addition to assessing the fixed component structure (leaf area index, pCO_2, and light) using the maximum likelihood estimation method (ML). Our output represents the response (pH, Ω_{Ar}, and pCO_2), estimation method, model, degrees of freedom (*df*), Akaike information criterion (AIC), Bayesian information criterion (BIC), logliklihood, Test, logliklihood-ratio (L Ratio), and *p*-value.

Response	Estimation	Model	*df*	AIC	BIC	logLik	Test	L Ratio	*p*-value
pH	REML	gls1	10	-57.14	-44.18	38.57			
		lme1	16	-47.91	-27.18	39.96	gls1 vs. lme1	2.77	0.837
	ML	gls1	10	-121.31	-105.47	70.65			
		gls2	9	-116.43	-102.18	67.21	gls1 vs. gls2	6.88	0.009
Ω_{Ar}	REML	gls1	10	7.54	20.5	6.23			
		lme1	16	16.09	36.83	7.95	gls1 vs. lme1	3.45	0.75
	ML	gls1	10	-35.06	-19.22	27.53			
		gls2	9	-34.02	-19.77	26.01	gls1 vs. gls2	3.04	0.081
pCO_2	REML	gls1	10	404.27	417.23	-192.13			
		lme1	16	414.38	435.12	-191.19	gls1 vs. lme1	1.89	0.93
	ML	gls1	10	493.91	509.74	-236.95			
		gls2	9	493.88	508.13	-237.94	gls1 vs. gls2	1.97	0.16

Table A10. Linear model summary output using generalized least squares for each response: pH (ΔpH Hr^{-1}), Ω_{Ar} ($\Delta\Omega_{Ar}$ Hr^{-1}), and pCO_2 (ΔpCO_2 µatm Hr^{-1}). The outputs show the factor, value, standard error (SE), t-value, and *p*-value.

Response	Factor	Value	SE	t-value	*p*-value
pH	(Intercept)	0.01	0.02	0.02	0.988
	LAI	0.02	0.01	1.17	0.059
	CO_2Enriched	0.06	0.03	1.96	0.060
	LightSaturating	-0.03	0.03	-0.92	0.367
	LAI:CO_2Enriched	-0.01	0.01	-0.46	0.648
	LAI:LightSaturating	0.05	0.01	2.17	0.039
	CO_2Enriched:LightSaturating	-0.03	0.04	-0.83	0.414
	LAI:CO_2Enriched:LightSaturating	0.03	0.02	1.27	0.215
Ω_{Ar}	(Intercept)	-0.09	0.06	-1.55	0.133
	LAI	0.04	0.03	1.42	0.167
	CO_2Enriched	0.21	0.09	1.24	0.064
	LightSaturating	0.07	0.09	0.74	0.465
	LAI:CO_2Enriched	-0.01	0.04	-0.33	0.743
	LAI:LightSaturating	0.11	0.04	1.61	0.019
	CO_2Enriched:LightSaturating	-0.13	0.13	-0.96	0.344
	LAI:CO_2Enriched:LightSaturating	-0.01	0.06	-0.07	0.944
pCO_2	(Intercept)	-18.69	43.75	-0.43	0.672
	LAI	-4.81	17.17	-0.28	0.782
	CO_2Enriched	-105.54	63.51	-1.66	0.108
	LightSaturating	19.35	61.87	0.31	0.757
	LAI:CO_2Enriched	87.12	19.64	-1.37	0.181
	LAI:LightSaturating	-61.75	24.29	-2.54	0.014
	CO_2Enriched:LightSaturating	116.05	89.82	1.29	0.207
	LAI:CO_2Enriched:LightSaturating	-19.79	42.12	-0.47	0.642

Table A11. Model selection for TCO_2, pH, Ω_{Ar}, and pCO_2 responses for the night-time trial (dark data). We compared models with full fixed effects (leaf area index * pCO_2 treatment, gls1) to models with leaf area index only (gls2). Here we report the degrees of freedom (*df*), Akaike information criterion (AIC), Bayesian information criterion (BIC), logliklihood, test, loglilihood ratio (L.Ratio), and *p*-value.

Response	Model	*df*	AIC	BIC	logLik	Test	L.Ratio	*p*-value
TCO_2	gls1	5	68.11	72.56	-29.05			
	gls2	3	69.25	71.92	-31.62	gls1 vs. gls2	5.14	0.076
pH	gls1	5	-131.63	-127.18	70.82			
	gls2	3	-121.97	-119.3	63.99	gls1 vs. gls2	13.66	0.001
Ω_{Ar}	gls1	5	-91.97	-87.52	50.99			
	gls2	3	-85.65	-82.98	45.82	gls1 vs. gls2	10.33	0.006
pCO_2	gls1	5	166.85	169.52	-80.43			
	gls2	3	162.26	166.72	-76.13	gls1 vs. gls2	8.59	0.014

Table A12. Dark data model summary (ΔTCO_2~LAI) including the factor, estimate, standard error (SE), t-value, *p*-value using the maximum likelihood estimation for only the dark data. The residual standard error was 1.378 on 18 degrees of freedom. These data were normalized by subtracting the mean of the control tanks (LAI= 0) from all tanks containing eelgrass. The mean ΔTCO_2 of the controls were 0.001 and -2.278 for the ambient (800 µatm) and enriched (1800 µatm) pCO_2 treatments respectively.

Response	**Factor**	**Value**	**SE**	**t-value**	***p*-value**
TCO_2	(Intercept)	-1.47	0.52	-2.84	0.011
	LAI	0.86	0.23	3.81	0.002
pH	(Intercept)	-0.003	0.002	-1.28	0.22
	LAI	-0.003	0.001	-2.5	0.024
Ω_{Ar}	(Intercept)	-0.01	0.01	-1.42	0.175
	LAI	-0.004	0.003	-1.3	0.211
pCO_2	(Intercept)	6.06	7.79	0.78	0.448
	LAI	8.38	3.42	2.45	0.026

Table A13. Initial conditions prior to the 1-hour incubation period for each treatment level of irradiance (saturating, sub-saturating and dark) (N=18 respectively) and pCO_2 treatments (ambient = 800 µatm and enriched = 1800 µatm) (N=10 and 8 respectively). Mean (± standard error) values of photosynthetic active radiation - PAR (mol m^{-2} d^{-1}), pH_T (total scale), total CO_2 (TCO_2 µmol kg^{-1}), and dissolved oxygen (mg DO L^{-1}). Water temperature (Temp. °C) and the change in water temperature during the incubation period (ΔTemp. °C) were averaged between irradiance treatments (N=18 respectively).

Irradiance Treatment	PAR (mol m^{-2} d^{-1})	pCO_2 Treatments	pCO_2 (µatm)	pH_T	TCO_2 (µmol kg^{-1})	DO (mg L^{-1})	Temp. (°C)	ΔTemp. (°C)
Saturated	9.16 ± 0.43	Ambient	795.8 ± 21.5	7.769 ± 0.016	2033.1 ± 2.8	10.37 ± 0.06	9.97 ± 0.06	0.68 ± 0.06
		Enriched	1778.89± 47.8	7.388 ± 0.013	2104.6 ± 11.2	10.31 ± 0.11		
Sub-saturated	2.59 ± 0.20	Ambient	750.8 ± 31.3	7.776 ± 0.017	2045.1 ± 6.1	10.27 ± 0.07	10.04 ± 0.05	0.47 ± 0.06
		Enriched	1822.6 ± 40.7	7.286 ± 0.015	2121.6 ± 4.0	10.29 ± 0.05		
Dark	0 ± 0	Ambient	775.8 ± 27.0	7.745 ± 0.001	2030.4 ± 4.6	10.48 ± 0.04	9.96 ± 0.03	0.31 ± 0.05
		Enriched	1858.0 ± 87.8	7.365 ± 0.020	2118.8 ± 4.2	10.49 ± 0.04		

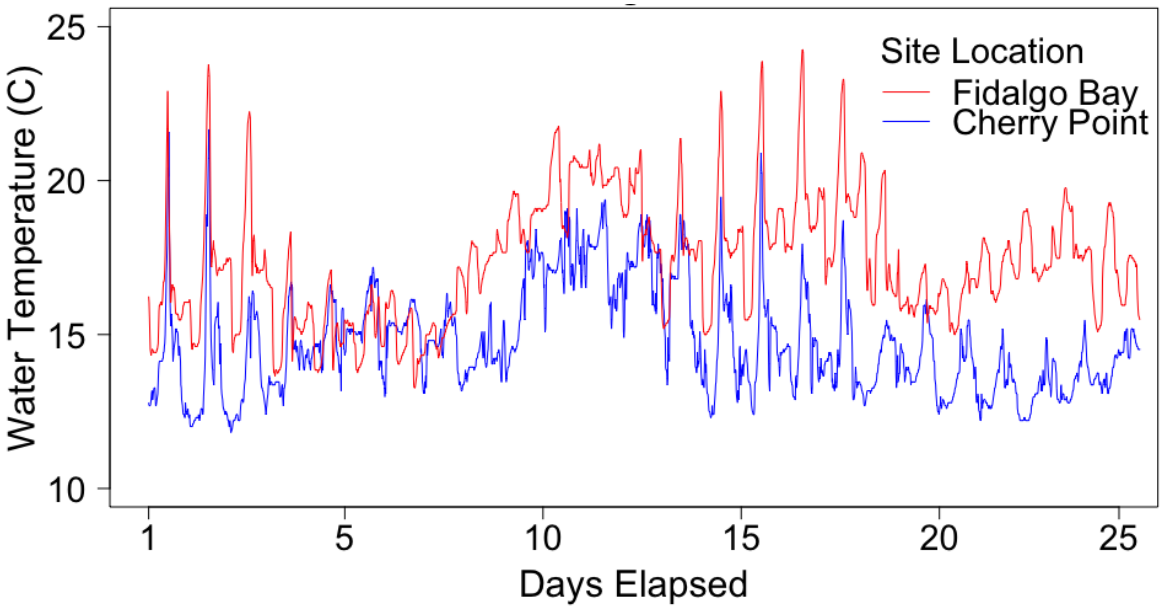

Figure A5. Changes in water temperature (°C) observed in the field across days elapsed. Measurements were taken in August, 2017 at Fidalgo bay (red line) and at Cherry Point (blue line).

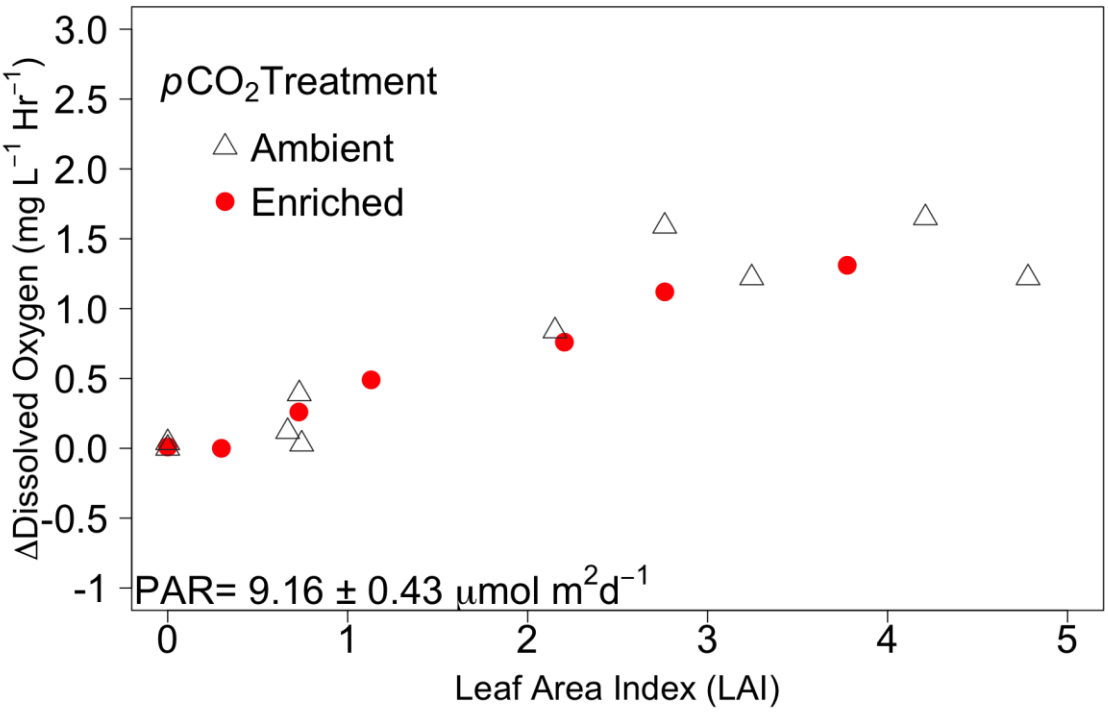

Figure A6. The change in dissolved oxygen (mg DO L^{-1} Hr^{-1}) over leaf area index (LAI) values. The black triangles represent ambient (800 µatm) and the red circles represent enriched (1800 µatm) pCO_2 treatments.